CHAPTER 4: Wave-induced water motion on shallow coral reef platforms

4.1 Introduction

Water motion is omnipresent in aquatic environments, particularly in shallow marine habitats (Denny and Wethey 2000). To be successful in these habitats, individual animals and plants must effectively interact with a great range of periodic, variable and sometimes extreme hydrodynamic processes dominated by waves (Denny 1988; Vogel 1996). In shallow marine communities, water motion is a fundamental factor in determining an individual's physiological, behavioural and biomechanical capability (e.g., feeding – Novell and Jumars 1984; Sebens 1991; respiration – Patterson et al. 1991; swimming – Wainwright et al. 2002; dislodgement – Massel and Done 1993). If an organism lives in a position where it does not receive its energetic requirements or is biomechanically vulnerable, then it must either move to another position (motile species) or risk detrimental consequences or mortality. Consequently, the spatial and temporal arrangement of sessile and mobile individuals in shallow marine communities will inevitably be determined, to various degrees depending on a range of life-strategies, by water motion (Done 1983; Lassig 1983; Connell and Keough 1985; Williams 1991; Witman 1992; Denny 1995; Bellwood and Wainwright 2001).

Due to the stochastic nature of the physical environment, water motion in shallow marine habitats is constantly changing and extreme hydrodynamic events that exceed organisms' physiological and biomechanical capabilities of an organism are a well-documented source of mortality (e.g., Dayton 1971; Paine and Levin 1981; Sousa 1984; Hughes and Connell 1999; Denny and Wethey 2000). If these events are a significant source of mortality in a community, as they commonly are in reef habitats (Woodley et

al. 1981; Lassig 1983), then they must be incorporated into an ecological framework in order to fully understand the community's dynamics (Sousa 1984; Denny 1995).

Despite our knowledge that water motion plays a crucial role in structuring shallow marine communities, we have limited capacity to quantitatively predict water motion at the full range of spatial and temporal scales important to individual animals and plants (Gaines and Denny 1993; Denny 1995). Often, empirical studies have taken too few measurements to provide the level of fine-scale spatial resolution needed to ascertain a hydrodynamic environment's physiological, behavioural and biomechanical consequences for reef organisms (Denny 1995). Moreover, data are often gathered in discrete temporal increments which do not span the full scale of an organism's lifetime (or even a significant portion thereof), and, furthermore, these data are rarely gathered during those disturbance events that are most likely to be the determinants of the organism's survival (e.g., cyclones and storms). Reef-scale oceanographic studies have typically focused on the retention and transport of reproductive propagules (Black and Gay 1990b) and the attenuation of wave energy spectra (Black 1978; Hardy and Young 1996). Physiologically and biomechanically relevant measures of water motion, such as maximum water velocity, are difficult to accurately extrapolate from these studies. Consequently, hydrodynamic environments on coral reefs tend to be characterised by coarse-scale categories (e.g., exposed versus sheltered) and generally do not provide specific quantitative data on the magnitude of differences in hydrodynamic exposure among categories. The aim of this chapter, therefore, was to present a comprehensive quantification of absolute, fine-scale water motion with which an individual organism is likely to interact on a typical exposed shallow reef platform during its lifespan.

Extreme levels of water motion in shallow marine habitats are produced almost exclusively by waves (Massel 1989; Gaines and Denny 1993; Komar 1997). Waves, in

most instances, are produced by wind blowing over the surface of the ocean (exceptions include geothermal activity). The higher the wind velocity, the longer the wind duration and the greater the distance over which the wind interacts with the ocean (the fetch), thus the greater the size of the resultant wave climate (see Komar 1997 for details). The wave climate is the sum of a large number of simple waves of differing heights and periods. The average of the highest third of these waves is known as the significant wave height (h_s) and together with the peak period (t_p, the dominant wave period within a wave climate's spectral density), these parameters adequately describe the size distribution of waves in a wave climate (Denny 1995). The additive nature of waves results in seemingly complicated ("bumpy") wave climates in which waves are continually moving in and out of phase. Nonetheless, the statistical nature of wave climates has been well described and, given a significant wave height and peak period, the expected return time of a given wave height can be predicted (Rayleigh 1880; Longuet-Higgins 1952; Eckart 1952; Denny 1988). Furthermore, by knowing the parameters of a wave climate (i.e., significant wave height and period) and its duration, useful attributes of the wave climate, such as the largest wave, can be accurately estimated (Denny and Gaines 2002).

As waves travel into shallower water, they undergo a series of gradual transformations (e.g., direction, wave velocity, height, energy, and others; see Komar 1997 for details). On coral reefs, however, a characteristically steep leading reef edge results in the continuation of untransformed large waves in the near-crest shallow water depths (Massel 1989). Conversely, such waves encountering a gently sloping beach profile or rocky shore would have already broken and thus been transformed in some or all of the aforementioned ways. The lack of transformation of incoming waves on a reef renders the reef crest a particularly hostile hydrodynamic environment for the

organisms that reside there.

As the wave travels from the reef crest over the reef, the wave's energy and subsequently its height, attenuates via two different processes: wave breaking and substrate friction. Wave breaking is the result of the reduction in wave velocity as its moves into shallow water and the resulting shortening of its wavelength and increase in height (Massel 1989). In this scenario, the front and back faces of the wave will steepen until a point where it becomes unstable and falls (breaks) (Denny 1988). These discrete events result in a large net loss of energy, and consequently the height of the wave continually diminishes as it propagates over the reef flat toward the reef back (Black 1978; Hardy and Young 1996). Energy loss to substrate friction is typically small on sandy beaches and is often ignored in wave models (e.g., Thornton and Guza 1983). However, on coral reefs, complex topographies cause pronounced frictional effects resulting in significant wave energy loss (Black 1978, Hardy and Young 1996). To quantify water motion spatially on a reef it is necessary to consider both forms of energy loss. By knowing changes in the height and period of waves as they propagate over the reef, one can calculate the maximum displacement, velocity and acceleration of water produced by these waves, and to which reef organisms are exposed (Denny 1988, 1995).

To quantify water motion spatially and temporally on a typical shallow coral reef platform, a 37-year historical dataset of wind was used to generate a 37-year history of wave climates impinging upon the study site at Lizard Island, the Great Barrier Reef (GBR), Australia. Equipped with the historic dataset, three objectives were undertaken in this study. The first objective was to use these historical data to predict the expected future return times of wave climates of varying magnitude and, therefore, estimate the recurrence of significant hydrodynamic events that constitute physical disturbance on

the study reef. The second objective was to statistically calculate the largest wave which will be expected to propagate over the reef during a given organism's lifetime. The third and final objective was to determine how a wave's height attenuates over the reef and how the associated levels of water motion (i.e. displacement, velocity and acceleration) change in accordance. With this knowledge, predictions can be made as to how waves act to shape a reef-scale hydrodynamic gradient.

4.2 Methods

4.2.1 Study location

The GBR lagoon is protected from large period oceanic swells due to a series of ribbon and patch reefs that have formed at the edge of the northeast Australian continental shelf (Fig. 4.2a). Although swell may permeate through these barriers via gaps and during high tides, it assumed that, due to attenuation, diffusion and diffraction, the oceanic contribution to the local wave climate is negligible. This assumption facilitates the calculation of wave climates within the lagoon based on local wind conditions.

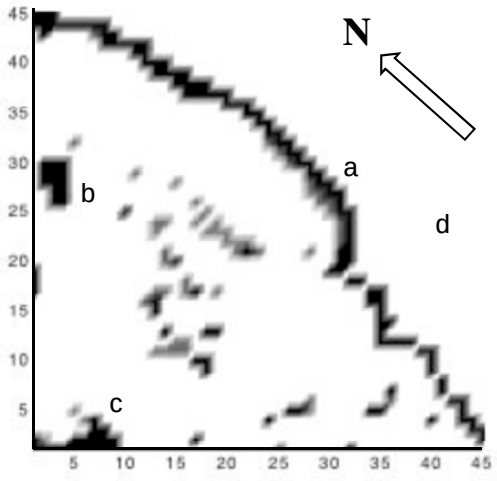

Fig. 4.1: A digitised map of the southeast Lizard Island and outer barrier ribbon reef region, the GBR, Australia, showing a) the ribbon reefs and edge of the continental shelf, b) Lizard Island, c) Cape Flattery (mainland Australia), and d) the Pacific Ocean. Each grid cell was 600 metres squared and depth averaged. Black shading corresponds to zero metres depth (lowest astronomical tide) and white shading corresponds to depth 20 metres or deeper.

The study was conducted on the exposed southeast reef at Lizard Island, Australia (Fig. 4.1b). For the majority of the year, prevailing south-easterly winds produce the wave climate at this site (Fig. 4.2) with fetches ranging from 10 to 40 km from the outer-shelf ribbon reefs to the study site depending on variation in wind direction (Fig. 4.1a). The southeast reef, like many in the GBR lagoon, rises steeply from a 20-30m depth to form a distinct reef crest, an extensive reef flat (approximately limited in vertical growth by the lowest astronomical tide, LAT) and a back reef that gradually subsides back to an intra-reefal lagoon.

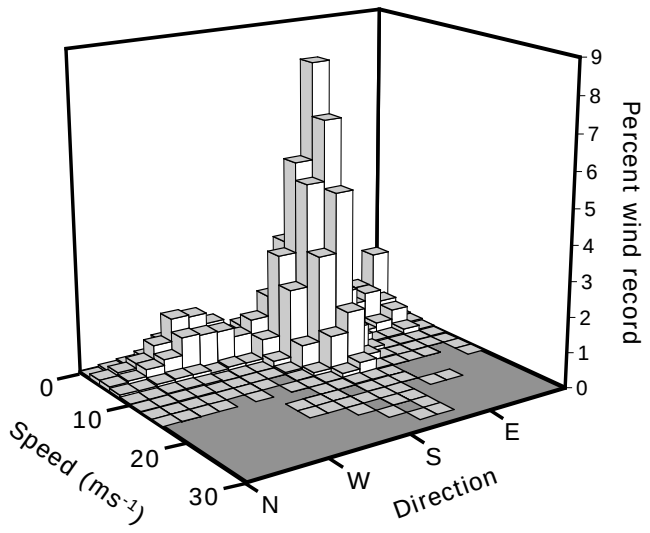

Fig. 4.2: The 37-year wind rose diagram of the Lizard Island area.

4.2.2 Expected return time of maximum significant wave heights

Locally generated wave climates (significant wave heights and corresponding peak wave periods) were predicted for the southeast Lizard Island area using a numerical wave generation model (WGEN) which was developed for fetch-limited water bodies (Black and Rosenberg 1993). The model incorporates depth-limited breaking, shoaling and substrate friction, which are essential factors dictating wave diffusion in areas containing islands and shallow water reefs. A 27 kilometre square area was selected

which encapsulated the body of water spanning from the southeast of Lizard Island to the outer ribbons reefs (Fig. 4.1). This area was divided into a 45 x 45 600-metre square cell bathymetry grid for digitisation (Fig. 4.1). Each of the digitised cells was assigned the cell-averaged depth to the closest 0.1m. Any cells below 20m were set to 20m because the interaction of the waves generated in the Lizard Island area with the bottom topography is insignificant beyond this depth (U.S. Army Corps of Engineers 1984). Cells containing depths of 0m (LAT) or less were considered impenetrable by waves (i.e., land and extremely shallow reef).

To assess the accuracy of the wave generation model, field measurements of wave climate were taken on seven separate occasions during January 2003 spanning a range of wind conditions. Measurements were taken approximately 50m seaward of the southeast reef in approximately 30 metres of water. Video footage was taken of a calibrated pole which was anchored so that a buoy attached to the bottom of the pole was submerged, thus forcing the pole to remain vertical (Fig. 4.3a). The water level on the calibrated pole was measured every 0.25 seconds to produce a 256-second time series of water level at each of the seven occasions. The wave climate records were decomposed using Fourier analysis and the significant wave height and peak period were calculated (see Black and Gay 1990). The hourly record of wind speeds and directions for the month of January at Lizard Island and the bathymetry grid were input into the wave generation model. The model then gave an output of predicted hourly significant wave heights and peak wave periods for the area directly offshore of the southeast reef which corresponded to the study site (Fig. 4.1b). The field measurements of significant wave height and peak period for each occasion were then plotted against model predictions for the same seven occasions for visual concurrence with the unity line (i.e., the line for which observed = predicted).

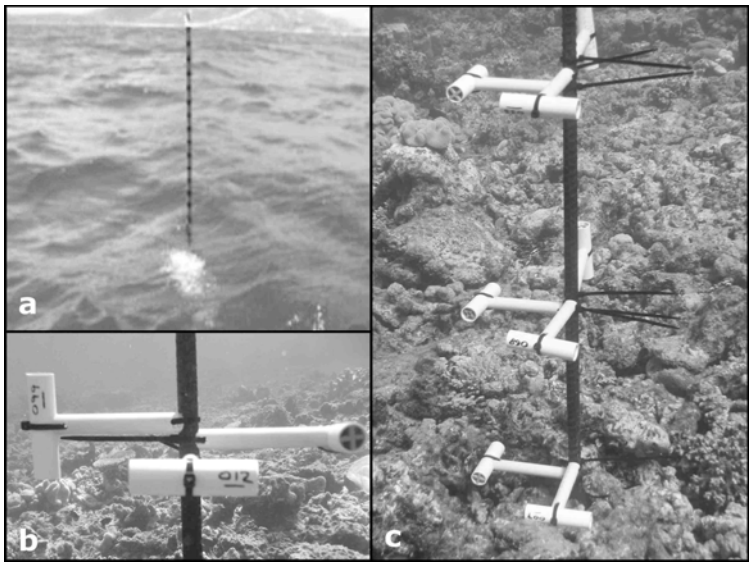

Fig. 4.3: a) Submerged anchored buoy and vertical calibrated pole for recording wave climate. b) and c) show different angles of the unidirectional plaster-type flowmeters.

Because the Lizard Island-specific wind record had only been maintained for six years prior to the study and many large data gaps were present within this record, a surrogate wind record was used for predicting historical wave climates. The Low Islets wind record, attained from the Australian Bureau of Meteorology (BOM 2003), was selected as this surrogate for three reasons. First, the Low Islets is the closest offshore weather station (180km south). Secondly, this record was the most similar to the Lizard Island record compared to a number of other geographically-close records that were considered. Yearly, monthly and weekly average wind speeds were indistinguishable between the Low Islets and Lizard Island wind records. Finally, the Low Islets record had been consistently maintained for the previous 37 years. Therefore, using hourly wind speeds and direction of this record, the wave generation model was used to predict a 37-year hourly history of significant wave height and corresponding peak wave period for the study site (i.e., a 37-year record of wave climates).

To calculate the expected return time of maximum significant wave height,

statistics of extremes were utilised (Gumbel 1958). The maximum significant wave height, $h_{s,max}$, for each year of the 37-year record were ranked and allocated an estimate of cumulative probability (see Denny and Gaines 2002), given by:

$$P(h_{s,\max} \le h_{s,i}) = \frac{i}{n+1}, \tag{4.1}$$

where $h_{s,i}$ was the magnitude of the maximum wave height of rank i and n was the number of maxima (n = 37). A maximum likelihood optimisation was used to find which of Gumbel's three asymptotic extreme value distributions best fit the ranked cumulative probability estimates. The Gumbel Type II distribution proved to be the best fit, and is given by

$$P(h_{s,\max} \le h_s) = e^{-\left(\frac{b_1}{h_{s,\max}+b_2}\right)^{b_3}} \tag{4.2}$$

The return time, t_r, (in years) was then calculated as

$$t_r = \frac{1}{1 - P(h_{s,\max} \le h_s)} \tag{4.3}$$

4.2.3 Expected largest wave during a given wave event

The 37-year record of wave climates was divided into what were called "wave events" which were periods of time within which the significant wave height did not vary appreciably. Wave events were thus defined as the period of time t (in hours) for which the average significant wave height for hours $t-1$, t and $t+1$ did not vary more than 0.1m from the average for hour $t-1$. Additionally, if the range of significant wave heights within a wave event ranged greater than 0.3m, a new event was started. Each wave event was assigned a significant wave height and peak period equal to the average outputs of the wave generation model for the duration of the event. This procedure smoothed irregularities in the wind record and avoided having to group events into

discrete wave climate bins.

The longer the duration of a wind event and the corresponding wave climate, the greater the chance that the various waves that make up the climate will align to produce a large wave. The height of the largest expected wave, h_{max}, in a wave climate with significant wave height, h_s, and peak period, T_p, for a given duration, t, is given by:

$$h_{\max} \cong \frac{h_s}{1.529}\left(\sqrt{\ln(t/T_p)} + \frac{\gamma}{2\sqrt{\ln(t/T_p)}}\right), \tag{4.4}$$

where γ is Euler's constant (adapted from Longuet-Higgins 1952; Longuet-Higgins 1980).

4.2.4 Expected largest wave during an organism's life

The largest wave that an organism is expected to encounter during its lifetime was estimated using the cumulative time spent within a series of variable-width wave climate bins (i.e., similar wave events). 10,000 hypothetical individuals for each of 25 ages (ranging between 1 day and 100 years old) were randomly placed on the 37-year record which was looped to simulate continuous time. The significant wave heights of wave events were categorised into wave height bins and the duration that each individual spent within each bin during its life was determined. The largest expected wave was then calculated for each bin using a randomly picked significant wave height drawn from within that bin (Eq. 4.4). The largest wave from all the bins that an individual lifespan covered was assigned as the largest wave the individual experienced during its life. For each age, the maximum wave heights for each of the 10,000 individuals were ranked and the wave heights corresponding to the median (50%) and 99th percentiles were plotted. This procedure was repeated for progressively narrower bins: as bin width approached zero, the expected maximum wave height experienced by

an individual colony of a given age converged on the optimal estimate.

4.2.5 Wave attenuation and water motion over the reef

The attenuation of waves and subsequent loss of height over the reef was calculated with the aid of a numerical model (2dBeach) that was developed for beach circulation and sediment transport (Black and Rosenberg 1992). In this model, the unsteady wave-height transformation equations were solved using a combination of Lagrangian and Eulerian methods which eliminated the numerical diffusion errors that are common to purely Eulerian solutions (Black and Rosenberg 1992). The Lagrangian scheme also effectively handled the sharp discontinuity in wave heights across the breakpoint on the reef. Importantly, the attenuation model considered loss of wave energy attributable to substrate friction, which is significant on coral reefs. An average reef depth profile (to the nearest 0.1m) was empirically constructed for the southeast reef at Lizard Island using three replicate profiles that were run from approximately 30m seaward of the reef crest to across the reef flat 600m to the back of the reef. The datum (0m) coincided with the reef crest which was defined as the point where the upper slope became approximately horizontal.

The wave attenuation model was calibrated using simultaneous field measurements of relative water motion over the reef. These field measurements were taken using unidirectional plaster-type flowmeters (Fig. 4.3b, c). These flowmeters were designed to halve their dry weight in 4 hours when exposed to hydrodynamic conditions similar to those at the reef crest during a wave climate of 1m significant wave height. Therefore, dry weight loss would generally range between 30-50%, approximately the percentage recommended for most accurate results when using plaster-type flowmeters (Hart et al. 2002).

Along three replicate transects 20m apart, steel bars were inserted vertically into the reef substrate at five stations: 0m, 20m, 40m and 60m from the crest and at the back of the reef (600m from the crest). Flowmeters were deployed for exactly 4 hours at times of constant wind speed and direction and when reef currents were minimal (i.e., less than $0.1ms^{-1}$). For this study, the flowmeters that were attached to each bar at 0.15m above the substrate and parallel with wave propagation in Fig. 4.3b were used for model calibration. The proportional weight loss was calculated using the initial and final dry plaster weight, and the three replicates at each station were averaged. Relative water flux was calculated as the fraction of averaged plaster loss at each station over the total loss for all stations.

Calibration of the wave attenuation model consisted of running the model using the significant wave heights and periods measured in the field and the hourly tide heights that corresponded with the seven dates and times when the flowmeters were deployed. The model predictions of relative water flux at distances over the reef corresponding to the flowmeter stations were then calculated. The model was parameterised by altering the substrate friction (a single constant for the whole reef) until predictions of relative water flux matched, as closely as possible, the flowmeter measurements. Once the model was calibrated, it was run at a number of prescribed significant wave heights and tide heights that were representative of the complete 37-year dataset (the full dataset could not be included due to computing limitations). Nonetheless, the attenuation of waves for all combinations of wave heights (0.5m, 1m, 1.5m, 2m, 4m and 6m) and tide heights (0m, 1m, 2m and 3m) were calculated.

The maximal horizontal water displacement, velocity and acceleration over the reef were calculated using linear wave theory (Denny 1988). When the substrate is at depth d from the still water level, and y is a distance above the substrate, the horizontal water

displacement x, velocity u and acceleration a (measured relative to the stationary substrate) for a given wave height H are, respectively:

$$x = \frac{-H}{2}\frac{\cosh(ky)}{\sinh(kd)} \tag{4.5}$$

$$u = \frac{\pi H}{T}\frac{\cosh(ky)}{\sinh(kd)} \tag{4.6}$$

$$a = \frac{2\pi^2 H}{T^2}\frac{\cosh(ky)}{\sinh(kd)} \tag{4.7}$$

where the wave number $k = \frac{2\pi}{L}$, and the wavelength $L = \frac{gT^2}{2\pi}\sqrt{\tanh\left(\frac{4\pi^2 d}{T^2 g}\right)}$.

4.3 Results

4.3.1 Expected return time of maximum significant wave heights

The wave generation model predictions of significant wave height and peak period were remarkably similar to those recorded in the field (Fig. 4.4a,b). The disparity between observed and predicted significant wave height was never greater than 4 centimetres for the range of wave climates tested. However, the predicted values of peak period were marginally, but consistently, lower than those measured in the field (by 0.5 seconds). The excellent congruence between the model and empirical data gave confidence that the model's predictions are reasonably accurate for the range of wind velocities and wind directions within the historic wind record.

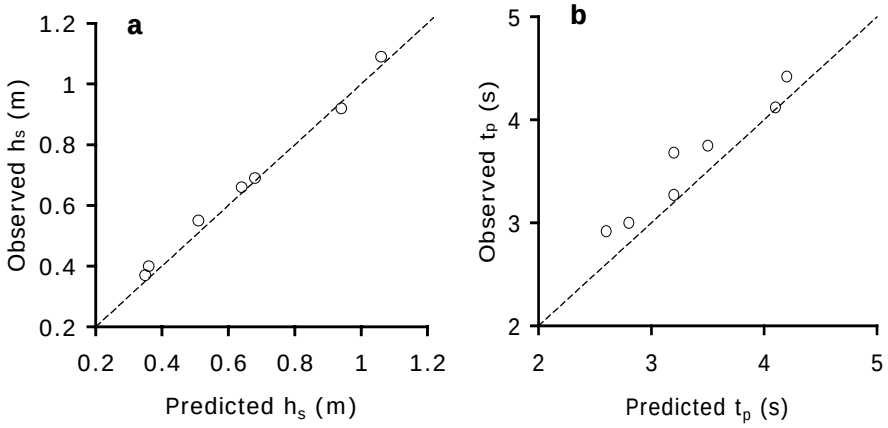

Fig. 4.4: Comparison of a) significant wave height and b) peak period for wave climates measured in the field (observed) and predicted by the wave generation model (predicted) at seven different wind events.

The higher ranks of the maximum yearly wave events corresponded with the timing of nearby cyclones and tropical depressions (Fig. 4.5a, Table 4.1). The highest winds recorded during the 37-year record were from cyclone Rona in February 1999, where wind speeds reached up to 27.8ms^{-1} (~56 knots or 100kmh^{-1}). Of the top seven wind events, Rona had the most variable wind direction, averaging approximately east-

southeast, producing seas with a predicted significant wave height of 2.55m. The second rank was cyclone Ivor, during March 1990, producing winds of up to 27.3ms^{-1} from the southeast and predicted seas of 2.50m. The top seven ranked wind events are summarised in Table 4.1.

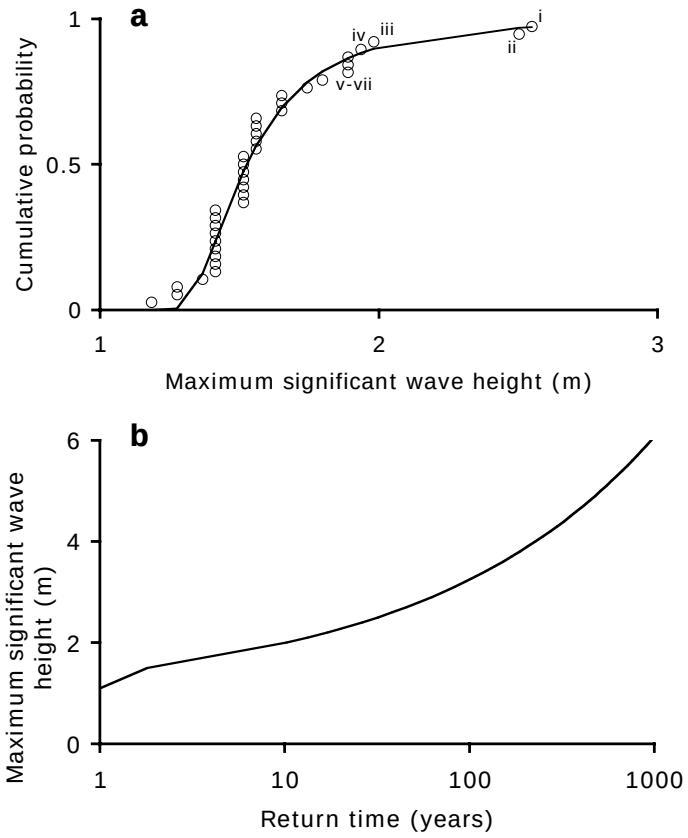

Fig. 4.5: a) Cumulative probability function of maximum significant wave heights for the 37-year wind and predicted wave record. See Table 1 for the seven greatest wave climates (i-vii). b) Return time of maximum significant wave height.

A Gumbel Type II cumulative probability curve best fit the ranked yearly maximum significant wave heights predicted from the 37-year wind record (Fig. 4.5a). The conversion of cumulative probability into expected return times of yearly maximum significant wave height facilitated the prediction of the largest wave climate that an organism is likely to experience during its lifetime on the southeast reef at Lizard Island (Fig. 4.5b). For example, an organism that lives for 20 years is expected

to encounter a wave climate with a significant wave height of approximately 2.1m or greater, whereas an annual organism is only expected to experience only a 1.1m or greater significant wave height during its lifetime.

Year	Cyclone name	Wind Speed (ms^{-1})	Wind direction	H_s (m)	T_p (s)	Duration (hours)	H_{max} (m)	Tide range (LAT)
1999	[i]Rona	27.8	ESE	2.55	5.86	12	5.1	0.7-2.2
1990	[ii]Ivor	27.3	SE	2.50	5.83	24	5.2	1.0-2.1
1997	[iii]Justin	21.6	SE	1.98	5.38	19	4.1	0.7-2.3
2000	[iv]Vaughan	21.1	SE	1.94	5.34	24	4.0	0.9-2.1
1973	[v]Unknown	20.6	SE	1.89	5.29	6	3.7	0.5-2.5
1986	[vi]Winifred	20.6	SSE	1.89	5.29	9	3.8	1.0-2.3
1989	[vii]Aivu	20.6	SE	1.89	5.29	3	3.5	1.9-2.7

Table 4.1: Summary of wind, wave and tide characteristics of the seven most severe wind events from the 37-year record at Lizard Island.

4.3.2 The expected largest waves through time

In the 37-year dataset, the median duration of historic wind events was 12 hours with 95% of the wind events between 1 hour and 3.4 days (81 hours) long (Fig. 4.6a). During the 37-year period, the longest wind event, which persisted for 16 days, averaged 7.7ms^{-1} (15 knots or 28 kmh^{-1}). Wind speeds of events over the 37-year period ranged from 0 to 27.8ms^{-1} with a median speed of 6.2ms^{-1}, and 95% of the wind events had speeds between 0 and 13.4ms^{-1} (~26 knots or 48kmh^{-1}). The corresponding predicted significant wave heights (from WGEN) averaged 0.56m with 95% of wind events, with significant wave heights ranging between 0 and 1.22m.

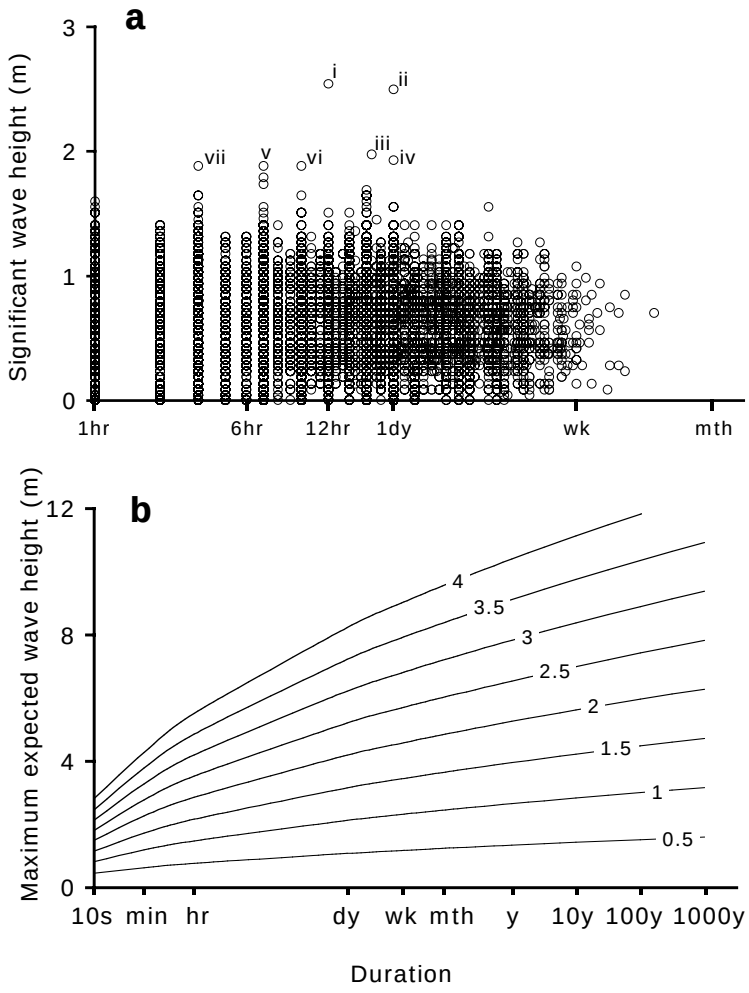

Fig. 4.6: a) Predicted significant wave height as a function of wind event duration (log-scale) from wind events of the 37-year record. See Table 1 for the seven greatest wave climates (i-vii). b) The maximum expected wave height as a function of wave climate duration (log-scale). Each solid line represents the significant wave height from a range of wave climates ranging from 0.5 to 4 metres.

In any 100-year period, the southeast reef at Lizard Island was predicted to encounter a wave between 4.5 and 5.5m high (Fig. 4.7), and a 100 year old organism will thus experience the water motion produced by such a wave. Over the past 37 years, the vast majority (99%) of 1-year old organisms are predicted to have experienced the effects of a maximum wave height between approximately 2 and 5m during their life.

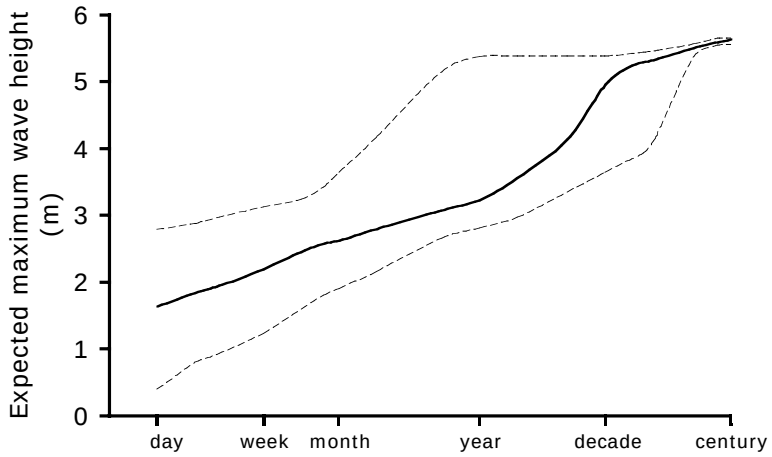

Fig. 4.7: The expected largest wave for a given duration on the southeast reef at Lizard Island. Solid line represents the median largest wave height and dashed lines the 99% confidence ranges.

4.3.3 Wave attenuation and water motion over the reef

The relative weight loss of unidirectional plaster flowmeters deployed during a range of wave climates and tide heights best fit the predictions of the wave attenuation model (2dBeach) when the reef friction constant was set to 0.16 (Fig. 4.8). A linear regression of observed versus predicted water flux confirmed excellent fit of the model to the data, with a slope not significantly different from one and an intercept not significantly different from zero (slope estimate = 1.07, $p < 0.000$, SE = 0.059; intercept estimate = 0.01, $p = 0.336$, SE = 0.013). Remarkably, a reef friction coefficient of 0.16 was also found by Black and Gay (1990) in a study investigating hydrodynamic mechanisms for crown-of-thorn starfish outbreaks on multiple reefs within the GBR lagoon. These similar best-fit values allowed for increased confidence that attenuation had been represented accurately by the value chosen for this coefficient.

As waves approach and propagate over the southeast reef at Lizard Island, a combination of shoaling, breaking and attenuation significantly alters their wave height

(Fig. 4.9) and consequently the maxima of associated displacements, velocities and accelerations of water near the substrate (Fig. 4.10). Sharp decreases in wave height and corresponding decreases in water motion (steep negative slopes in Figs. 4.9 and 4.10) correspond to attenuation caused by wave breaking. Waves break for all wave heights at extreme low tide (LAT), although the breaking gradient becomes steeper for larger waves and probably represents a continuum from a spilling to a "sucking and plunging" breaking formation (Denny 1988). The larger the wave, the higher the tide at which breaking can occur, and for 4 and 6m waves, breaking occurs at a 3m tide (note that the highest recorded tide at Lizard Island over the 37 years was 2.9m). Gradual decreases in wave height correspond to attenuation caused by reef friction and are most marked at low tides. This pattern is clearly illustrated at lower wave heights where reef friction attenuation was greater at lower tides (Figs. 4.9 and 4.10). Frictional attenuation is less dominant for larger waves because retention of high wave periods facilitates faster wave progression over the reef.

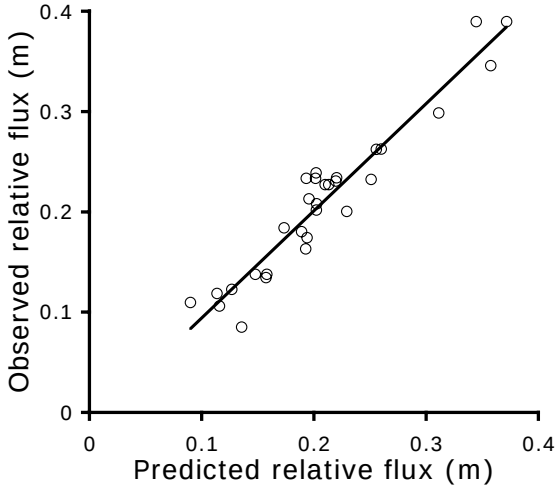

Fig. 4.8: Relative water flux measured in the field (observed) and relative water flux predicted by wave attenuation model (predicted) during the above seven wind events and corresponding tide heights. A linear regression line illustrates the fit of the model with a reef friction coefficient of 0.16.

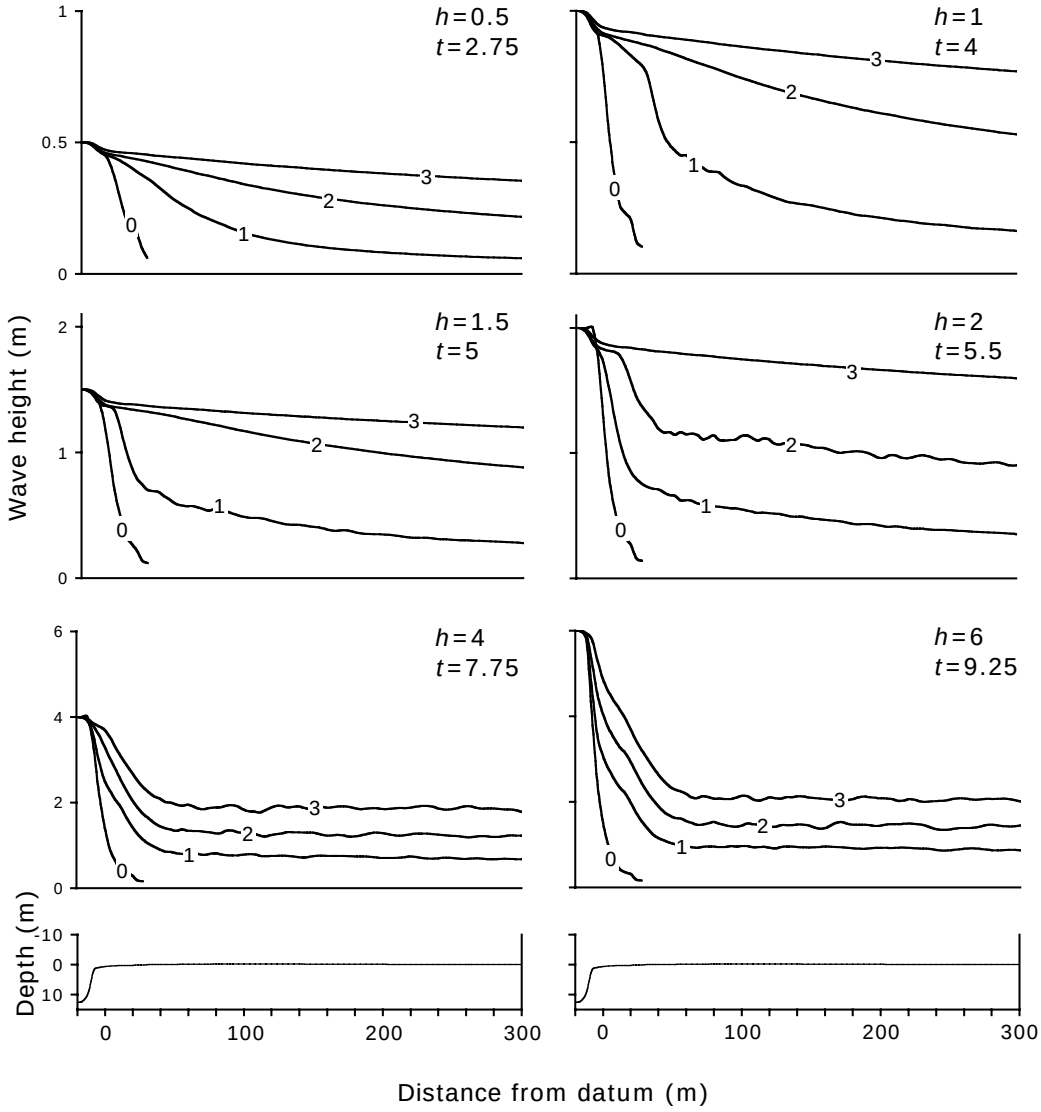

Fig. 4.9: Predicted change in height on waves (h=0.5, 1, 1.5, 2, 4, 6m and corresponding periods in seconds) across the reef profile (given at base of figure) at the southeast reef at Lizard Island. Individual lines represent 0, 1, 2 and 3m tides. Steep negative slopes indicate wave breaking and gradual slopes indicate attenuation through reef friction.

During the time it takes for a wave to pass a given position on the reef, the level of each component of water motion (displacement, velocity and acceleration) ranges from zero to its maximum value. These maximum levels (for displacement, velocity, and acceleration) change differentially as a function of wave height (Fig. 4.10). In this figure, the velocity scale is kept constant in all graphs (i.e., the middle scale bar is consistent across all figure panels). As wave height increases, the displacement scale

contracts (i.e., the scale bars become shorter). This indicates that water displacement increases at a greater rate than water velocity as wave size increases. For example, maximum velocity at the reef crest undergoes an 8-fold increase between wave heights 0.5 and 6m, whereas maximum displacement undergoes a 30-fold increase per wave cycle. Conversely, water acceleration changes to a lesser degree than the other two components of water motion as waves get larger, and this phenomenon is illustrated by an increase in scale with increasing wave height.

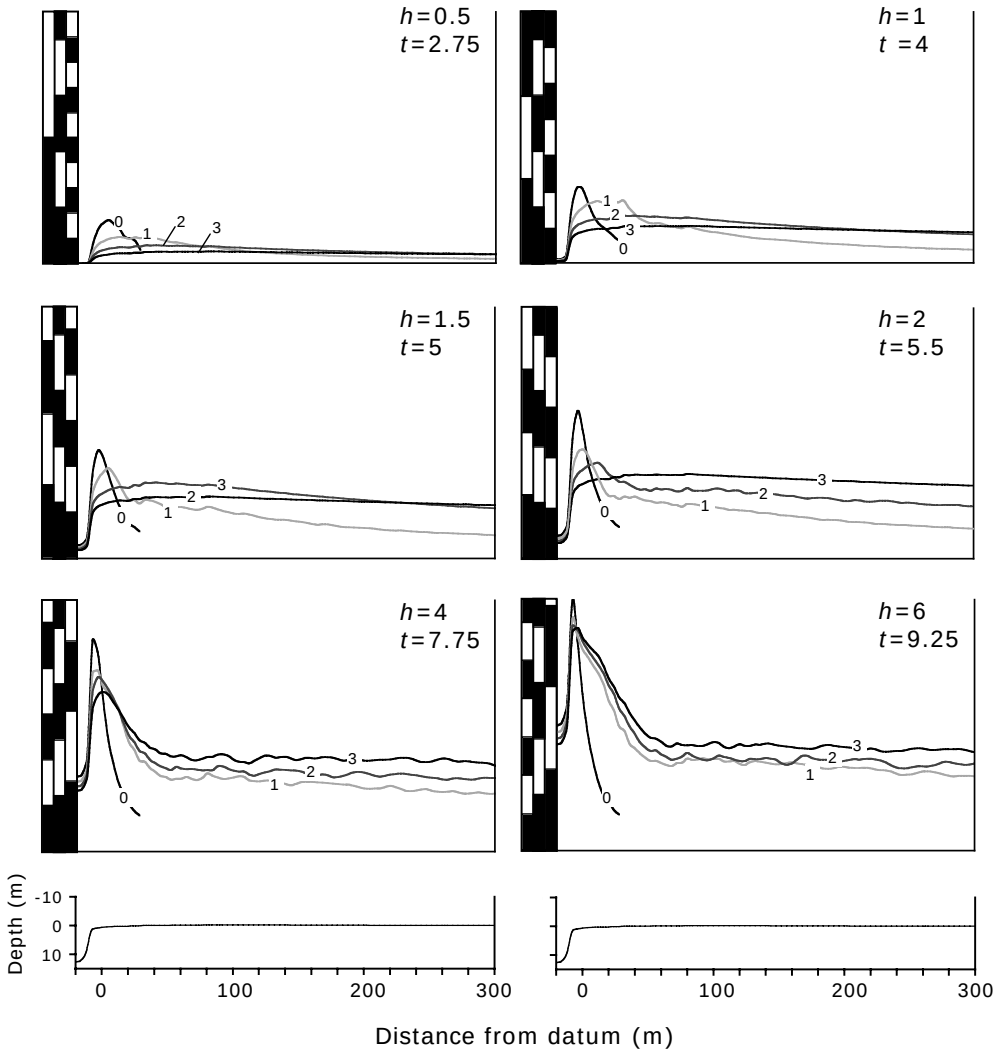

Fig. 4.10: Predicted maximum horizontal water motion across the reef profile (illustrated at base of figure) for the same wave heights and periods as Fig. 4.9. Scale bars (from left to right) represent one unit of displacement (m), velocity (ms^{-1}) and acceleration (ms^{-2}) respectively. Individual lines represent 0, 1, 2 and 3m tides.

The position of maximum hydrodynamic action on the reef varies depending on the combination of wave and tide height. For extreme low tides, the maximum displacement, velocity and acceleration of water consistently occurred at the reef crest, although at greater wave heights this maximum moved progressively offshore due to the increased breaking depth with increasing wave height. Note that the termination of the lines at 28m from the crest was due to water depth reaching zero for this tide height. As tide height increased, the point of maximum hydrodynamic action shifted across the reef. The distance from the crest of maximum water motion was smaller for larger waves, whereas the distance became indistinguishable for 6m waves between the different tide heights.

Although the combination of large waves and low tides produced the greatest water motion at the reef crest, these two factors reduced the magnitude of water motion further back from the crest. For example, a 2m wave at lower tides produced the highest levels of water motion at the crest, and due to breaking and bed friction, the lowest levels of water motion over the reef flat. Conversely, for the same wave height, higher tides (where breaking and frictional attenuation are reduced) allowed waves to propagate further over the reef, thus producing higher relative levels of water motion further from the crest. It can therefore be concluded that large wave climates may be detrimental to the reef crest area, but have less negative influence on reef flat and back areas. Conversely, intermediate waves at higher tides will cause higher degrees of water motion further back on the reef.

4.4 Discussion

Armed with a 37-year historic record of wind in the study region and two oceanographic models, this study estimated temporal and spatial levels of absolute water motion on a typical exposed coral reef platform in the GBR lagoon at scales ranging from seconds to decades and metres to an entire reef. The results of this study provide estimates of water displacement, velocity and acceleration at positions along a continuum of coral reef habitat, as well as descriptions of how the magnitudes of these three components of water motion vary through time. These results, discussed further below, have important implications for sessile animals and plants living along this habitat continuum.

4.4.1 The return-time of large wave climates

The return-times and magnitudes of wave climates that impinge upon shallow reef habitats have profound effects on the structure and dynamics of local communities (Dayton 1971; Paine and Levin 1981; Dollar and Tribble 1993; Connell et al.1997; Hughes and Connell 1999; Denny and Wethey 2000). This study illustrated that the larger of these wave climates at Lizard Island are associated with nearby tropical depressions and cyclones (Fig. 4.6a and Table 4.1), which are a typical phenomenon on the GBR (Massel and Done 1993; Nott and Hayne 2001). The cumulative probability curve of yearly largest wave climates derived from the 37-year record had no well-defined upper bound, indicating that larger seas are less likely to occur, but also that no significant wave height exists for which the likelihood of occurrence goes to zero (Fig. 4.5a). Interestingly, however, Lizard Island had not been directly intercepted by a cyclone during the 37-year record and therefore this probability curve may be

incomplete – the closest cyclone, Rona in 1999, passed at closest approximately 200km to the north and was a moderate category 3 on the Saffir-Simpson scale (BOM 2003). Thus, while a limit to wave climate size probably does exist in the GBR lagoon (due to increasing dissipation of wave climates with increasing wave climate size; Komar 1997), this limit would not have been attained in the 37-year record.

4.4.2 The largest waves on the reef

The likelihood of a larger wave in a Rayleigh distributed wave climate increases as a function of time (Denny and Gaines 2001). That is, the longer the cumulative duration of a given significant wave height, the greater the largest expected wave encountered will likely be. Fig. 4.6b shows this relationship theoretically for significant wave heights between 0.5 and 4m at Lizard Island. By repeatedly placing a given length of time randomly onto the 37-year record of wave climates and summing the time spent in different wave climates, this study estimated the largest expected wave that an organism is likely to encounter the reef during the specified length of time (Fig. 4.7). This figure indicates, for example, that if the reef crest at the southeast reef at Lizard Island was observed for one day, the smallest "large-wave" expected to encounter the reef would be on average approximately 1.6m high, although 99% of one day long intervals observed will contain a largest wave ranging between 0.3 and 2.7 metres. During longer periods, the largest expected wave height increases, producing an untidy relationship between observation time and wave height which is a reflection of temporal patterns inherent in the wind record. Although the wait times between large-scale meteorological processes typically approximate a Poisson processes (where events are random and independent; Spiegel 1993), the restriction of cyclones to summer months produces an obvious pattern. The increasing chance of intercepting a

cyclone's wave climate as periods approach one year is reflected in the upper 95% confidence interval. For example, if observing the reef for longer than a year, the chance of avoiding a cyclone becomes progressively smaller and the mean largest expected wave increases sharply (Fig. 4.7). The longer an organism lives on the reef, the larger the wave it is expected to encounter, however the hydrodynamic influence of this wave on the organism will depend upon its relative position on the reef and will be discussed below.

4.4.3 The attenuation of waves over the reef

The height of waves decrease over reef platforms due to a combination of reef friction and wave breaking which, in turn, are a function of water depth over the reef (tide) and wave parameters (height and period). Despite the excellent reef-averaged concurrence of the reef friction coefficient with Black and Gay (1990), substrate friction is likely to vary from reef to reef based on topographical, ecological and biological factors and, additionally, friction will vary on the same reef due to spatial variations in these factors. For example, reef habitats with low live coral cover will contribute less to the attenuation of waves compared to a habitat with high coral cover, and consequently, waves will retain a greater height as they propagate over the reef (Hardy and Young 1996).

Breaking causes waves to lose energy much more rapidly than substrate friction does (Fig. 4.9). However, because breaking events are discrete and substrate friction is continuous, the relative contribution to wave attenuation of these two processes will depend on the wave climate, reef dimensions and tide height. At low tide, for example, a large wave will lose the majority of its energy to wave breaking at the crest (e.g., Fig. 4.9, $h = 6$), whereas a small wave climate that does not break at the crest will lose the

majority of its energy to the continuous effects of reef friction (e.g., Fig. 4.9, $h = 1$). Except for rare periods of extreme low tide, the gradient in levels of water motion over the reef will increase with the size of the wave (Fig. 4.9). Therefore, during a typical day (modest tidal range and wave climate), hydrodynamic conditions will vary little over the reef. During more severe wave climates, an increasingly pronounced gradient of water motion between the reef crest and flat will emerge.

4.4.4 The motion of water on the reef

The three components of water motion on coral reefs are highly variable, yet are spatially and temporally predictable as waves propagate over the reef. Typically, a gradient in water motion exists where motion is greatest near the reef crest and lessens toward the back of the reef (Fig. 4.10). However, during combinations of intermediate to high tidal levels and low and intermediate wave heights, the position of maximum water motion can form a substantial distance shorewards from the crest. However, during significant hydrodynamic disturbance events - those likely to significantly influence community structure - this gradient is most pronounced over the leading 60 metres of exposed reef (Fig. 4.10).

Of the three components of water motion, displacement varied the greatest as a function of wave height. For small waves (e.g., 0.5m high), maximum displacement ranged between approximately 0.1 and 0.5m per cycle. However, for a 6m wave propagating over the reef, displacement ranged from approximately 3 to 6.5m per cycle. It is important to note that displacement is the maximum horizontal distance that a water particle has moved from a stationary position on the reef and that this particle will return to its initial position during the same wave cycle. Therefore, the actual distance of water that passes a stationary point on the reef is twice the displacement. While

displacement may be relatively small per wave cycle, formidable directional motion exists in marine habitats when considered in terms of absolute displacement per unit time. For example, during a typical daily wave climate of 0.5 metres (significant wave height), the displacement of water past a stationary point on the reef ranges between 5 and 20km per day depending on the tide height (Fig. 11a, calculated using the root mean square wave height, a tidal range between 0.5 and 2.5m, a wave breaking criterion of 0.78 and Eq. 4.5). For a typical 2m-wave climate on coral reefs (note that this is the significant wave height, not individual wave height), this range is approximately 25 to 40km per day. For a sessile organism, the quantity of food and other resources that it acquires is related to displacement (Nowell and Jumars 1984), so the greater the absolute displacement of water the greater the potential resources acquired.

Mobile organisms, such as reef fishes, may extend the minimum amount of energy needed to maintain their position on the reef by sitting passively in the water column. However, to intercept food or remain in the proximity of shelter (e.g., juvenile reef fishes), the animal may be required to swim considerable distances. Stobutzki and Bellwood (1997) discovered that late pelagic stage reef fishes could swim up to an average of 11.7 km per day before exhaustion. Assuming the distance that younger animals venture from shelter (e.g., a coral colony) is smaller than that of older animals, it is a possibility that the excellent swimming ability of juvenile reef fishes is a direct consequence of the necessity to maintain position in hydrodynamic reef habitats when they later settle on the reef.

In the absence of a strong boundary layer in wave swept habitats (Vogel 1996), differences in the magnitude of water motion at different vertical distances from the substrate at any point on the reef are small and, in most cases, insignificant on shallow reef platforms (Fig. 4.11b). For example, if the depth of water on the reef were three

metres, the differences between the substrate and at the water surface in horizontal displacement, velocity and acceleration values are all consistently around 0.3 units (m, ms^{-1} and ms^{-2}, respectively, Fig. 4.11b, calculated using Eq. 4.5, 4.6 and 4.7). The proportional value of this difference varies, however, depending upon the absolute values of water motion. For example, for small waves (less than 1m), this difference constitutes an approximate 50% difference in horizontal water motion, however for larger waves (greater than 1m), this difference becomes a progressively smaller fraction of the water motion (see Fig. 4.11b). Because intermediate to large wave heights are the most likely to be a mechanical threat to reef dwelling organisms, changes in levels of water motion as a function of height above the substrate can be ignored.

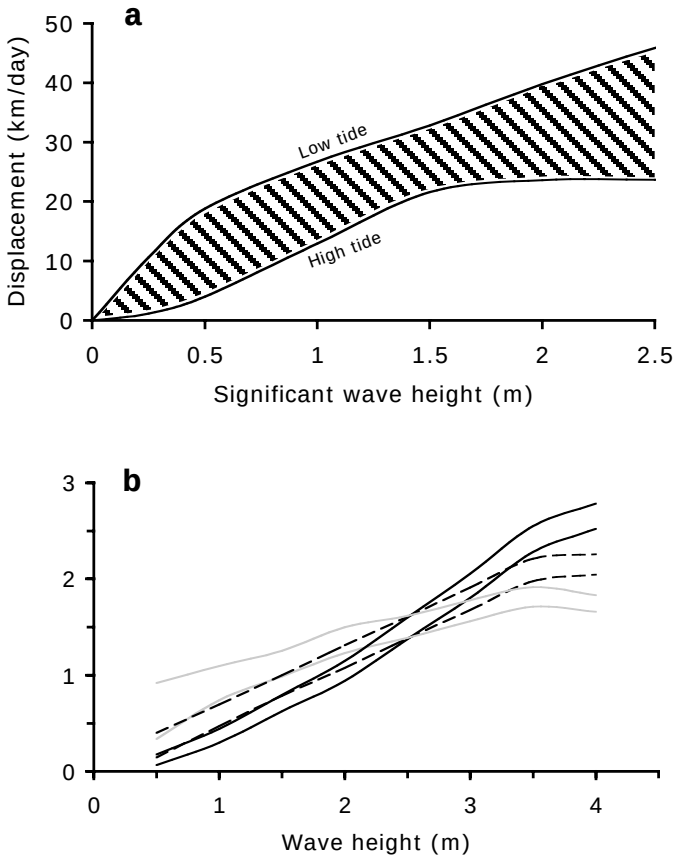

Fig. 4.11: a) The absolute water displacement above the substrate as a function of significant wave height. Shaded region representing the variation in absolute displacement associated with tide height (0 to 3m). b) The difference in displacement (solid black lines), velocity (dashed lines) and acceleration (solid grey lines) at the substrate (lower of paired lines) and water surface (upper of paired lines) at a water depth of 3 metres above the reef as a function of wave height.

Using known physiological, behavioural and biomechanical information on the optima and limitations of organism under varying levels of water motion, the approach used in this chapter lends greater insight into the potential spatial distributions of sessile reef organisms as a function of hydrodynamic environment. Of particular interest in understanding reef community dynamics in this context is the group of species which forms the primary habitat structure on reefs, the reef corals. These colonial animals are potentially dislodged during hydrodynamic disturbance events (Woodley et al. 1981;

Massel and Done 1993; Rogers 1993) and differential mortality is likely to be based on varying mechanical tolerances of this morphologically diverse group (Chamberlain 1978; Graus et al. 1977; Vosburgh 1981). Although the results presented in this chapter will be used in the next chapter to estimate spatial mortality rates of coral colonies on tropical coral reefs, the approach used to quantify water motion at various spatial and temporal scales presented in this study is transferable to other aquatic environments in which organismal success is related to water motion.

CHAPTER 5: Hydrodynamically induced mortality rates of reef corals

5.1 Introduction

Mortality is a highly variable process in biological communities (Connell 1972; Paine 1974; White 1979; Lubchenco 1980; Denny 1995). Untangling the myriad of mortality agents and their relative effects on individuals at scales relevant to the dynamics of a community is a difficult task, particularly since these agents and their relative effects vary greatly between study systems (Paine and Levin 1981; Sousa 1984; White and Pickett 1985). In sessile space-limited assemblages, such as coral reefs, rocky shore and terrestrial forests, the distinctions between mortality agents acting at different scales is more easily discernable than for other groups of organisms (Dayton 1971; Menge 1976; Connell 1979; White and Pickett 1985). Following habitat selection, small-scale, day-to-day mortality events tend to divide the community into zones (e.g., composed of organisms with similar physical and physiological tolerances, but also controlled to varying degrees by competitive and predatory interactions) that are periodically culled, or in some cases reset to earlier successional stages, by larger-scale disturbances such as temperature anomalies and extreme hydrodynamic events (Connell 1978; Hughes and Connell 1999). These large-scale, unpredictable, perturbations can potentially alter community structure (Knowlton 1992; Dollar and Tribble 1993; Rogers 1993). Furthermore, a community's structure is generally shaped by not only individual events, but also by the historical occurrences and interactions between sequences of disturbances (Hughes 1989; Tanner et al. 1996; Hughes and Connell 1999).

Reef corals potentially compete for space in the reef habitats for which they form the primary habitat structure (Lang and Chornesky 1990). Given sufficient time without disturbance, competitively dominant species can monopolise habitat and diversity tends to decrease (Connell 1979). Moreover, the diversity of associated interstitial species, such as mobile animals, also decreases (Menge 1976; Connell 1979; Bell and Galzin 1984; Stimson 1985; Williams 1991). However, coral reef communities rarely reach climax states (Rogers 1993; Connell et al. 1997; Hughes and Connell 1999). Furthermore, corals rarely cover all of the available substrate in a habitat (e.g., Tanner et al. 1994). Recurrent large-scale disturbance processes and recruitment limitation are two potential mechanisms which prevents corals from dominating reef communities (Hughes and Connell 1999; Hubbell 1999). Although "background" biological mortality is ubiquitous (e.g., chronic mortality due to competition, predation and disease), the maintenance of community structures in open space-dominated states is also strongly influenced by large-scale disturbance regimes (Sousa 1984). Therefore, to accurately project the dynamics of a coral reef community, it is necessary to understand and quantify the effects of these large-scale disturbances on community structure.

Elevated hydrodynamic events are recognised as one of the most important large-scale disturbance processes that alter assemblages of structural species on coral reefs (Connell 1978; Woodley et al.1981; Sousa 1984; Dollar and Tribble 1993; Rogers 1993). In hypothetical terms, a disturbance that affects all species equally would reduce cover, but overall community structure would remain the same (Hughes and Connell 1999). However, mechanical divergence and patterns of depth distribution in structural species causes physical disturbances to impose selective mortality. On coral reefs, competitively dominant species typically growth into mechanically vulnerable

morphologies and overtop neighbouring colonies (Wethey and Porter 1976; Jackson 1979; Stimson 1985), thus limiting the light available to the overtopped neighbours and further reducing their competitive ability. Because of this strategy, however, hydrodynamic disturbance events typically remove the competitively dominant species more frequently, and thus create space in which other species can settle (Connell 1978). However, the fates of individual coral colonies during a hydrodynamic disturbance, and subsequently the ways in which communities change based on their initial cache of mechanically diverse structural species, is largely unknown. Moreover, the predictability of the effects that hydrodynamic disturbances have on structural reef species before the events occurs have been largely overlooked, and therefore predictions of community change during future disturbances remain speculative.

In this chapter, I use a novel approach to predict dislodgement rates of reef corals on a typical wave-exposed reef in the GBR lagoon. Three factors are central in determining if a coral colony will be dislodged during a hydrodynamic disturbance (Chapter 2): 1) the limiting strength of the materials at the colony/substrate interface, 2) the maximum horizontal flow velocity produced by a passing wave and 3) the shape of the colony's projected area perpendicular to this flow. For a colony under the influence of velocity-induced drag force, the maximum stress, which is the force per unit area, occurs at its basal attachment surface and is a function of the colony's shape (Chapter 2). If the flow velocity reaches the point where the resultant maximum internal stress is greater than the strength of the reef substrate, the colony will be dislodged.

A comparison of the relative strengths of coral skeleton and the reef substrate shows that the substrate was consistently weaker than coral skeleton and was therefore the limiting material at the colony/substrate interface (Chapter 2). Furthermore, the substrate strength was highly variable at the scale that it was measured (< 1 cm^2).

Nonetheless, the local mean substrate strength provides a reliable estimate of a colony's limiting strength at the scale of the colony (Chapter 2). Substrate strength and flow velocity are two key aspects of a colony's external environment and were the focus of Chapters 2 and 4, respectively. Chapter 3 described the third key factor, the projected shape of a colony. This characteristic determines the degree to which hydrodynamic water velocity is translated as mechanical stress at the colony/substrate interface and is a variable upon which the animal exerts some degree of ecological and evolutionary control (Kaandorp 1999). Chapter 3 also developed a technique for predicting the maximum stress within a colony's base as a function of water velocity. The "maximum predicted stress" (MPS) is an estimation, based on classical engineering theory (Wainwright 1979; Denny 1988), of the maximum stress in the base of a colony per squared unit of water velocity (see Chapter 3 for details; Eq. 3.2). This quantity can be calculated for any rigid structure with knowledge of its projected shape perpendicular to horizontal water flow and the dimensions of its basal attachment area. With knowledge of the maximum velocity of water at a point on a reef where a colony resides and the strength of the substrate to which the colony is attached, one can derive the threshold MPS at which a colony is predicted to be dislodged (Chapter 3, Eq. 3.4). Conversely, knowing the strength of the substrate $\sigma_{substrate}$ and the MPS of a colony σ_{mps}, the threshold water velocity u_{thresh} above which the colony is dislodged can be calculated as:

$$u_{thresh} \geq \sqrt{\frac{\sigma_{substrate}}{\sigma_{mps}}}. \qquad (5.1)$$

Because maximum water velocity (per wave cycle) on the reef is implicitly related to local meteorological conditions (Chapter 4), and because large-scale meteorological phenomena can typically be modelled as Poisson processes (Spiegel 1992), it follows that waiting times between water velocity events great enough to cause colony

dislodgement are exponentially distributed. That is, chronic low intensity events are more predictable compared to high intensity events that occur in an approximately random and independent fashion. The rate parameter of a Poisson process can be estimated by fitting an exponential probability function to the waiting times between events (Spiegel 1992) such as the hydrodynamic disturbance events that cause mortality on a coral reef. If the exponential function fits the data well, the mean intrinsic (or instantaneous) rate of mortality for that colony can be estimated.

Using a 37-year dataset of hourly maximum flow velocity over the exposed southeast reef at Lizard Island, this study calculated the predicted instantaneous rates of mortality for coral colonies based on their MPS and the strength of the substrate at the position over the reef where they are attached. This approach resulted in a "contour map" of expected colony dislodgement rates as a function of mechanical vulnerability over the reef. Additionally, to illustrate the utility of the framework presented in this thesis, the estimated mechanical thresholds expected in one year and in 37 years were projected onto empirically-derived MPS levels of three coral populations living on the reef. These three species have different growth forms and therefore the projected mortality varied substantially. The competitively dominant species, *Acropora hyacinthus*, was shown to be significantly more vulnerable to hydrodynamic force relative to the competitively subordinate species (*Acropora palifera* and *Acropora gemmifera*), thus illustrating the potential importance of disturbance in restricting competitive exclusion on the study reef at Lizard Island.

5.2 Methods

5.2.1 A 37-year estimate of maximum flow velocity over the reef

A 37-year record of hourly wind speed and direction of the Lizard Island area was used to back-project a 37-year record of wave climates in the open water adjacent to the exposed southeast reef at Lizard Island, Australia (see Chapter 4 for details). The predicted record of wave climate was then divided into wave events, which were defined as the durations within which the wave climate's significant wave height did not change appreciably (see Chapter 4 for details). The largest expected wave during a wave event was calculated based upon the event's significant wave height, peak period and the duration of the event (Chapter 4; Denny and Gaines 2001).

The change in height of the largest wave as a function of distance over the reef was calculated using an empirically-calibrated wave attenuation model (see Chapter 4 for details). Using estimates of the wave parameters (i.e., maximum wave height and peak period) and the depth profile of the reef, the maximum horizontal flow velocity was calculated using linear wave theory (Chapter 4; Denny 1988). This calculation resulted in a comprehensive estimation of maximum water velocity for the past 37-years ranging spatially from the reef base (-24m from the reef crest) to 600m over the reef flat towards the Lizard Island lagoon (see Fig. 5.3b for reef profile).

5.2.2 Substrate strength over the reef

Replicate measurements of substrate strength over the southeast reef were taken using the geomechanical technique and field design outlined in Chapter 2. In summary, the tensile strength of the hard non-living reef substrate was measured 10 times at 30 replicate points parallel to the reef crest at 0, 40, 80, 120 and 600m from the reef crest

(0m) shoreward over the reef flat. An equation estimating the continuous change of average substrate strength over the reef was established by fitting a range of non-linear curves to the results using standard least square interpolation (Chapter 2).

5.2.3 Instantaneous rate of mortality

The instantaneous rate of mortality was predicted by fitting an exponential probability density function to the frequency distribution of the waiting times between wave events that would theoretically dislodge a colony of a given MPS value. The exponential distribution of waiting times between successive mortality events is

$$P(t) = \mu e^{-\mu t}, \qquad (5.2)$$

where t is time and μ is a fitted parameter. For an exponential distribution, $1/\mu$ is the expected time between events, and thus μ is the instantaneous rate at which disturbances occur (Spiegel 1992). The exponential probability density function was fitted using maximum likelihood (function "optim" in the software package R). Because the model exhibited good fit to the data, the exponential distribution coefficient μ was considered to be an accurate estimate of the Poisson disturbance rate or, in the case of coral colonies, the instantaneous rate of mortality from disturbance.

To illustrate changes in estimated mortality rate over the reef for a given colony, a contour map was created in which each contour referred to a prescribed colony MPS value. Because of the wide range of growth forms exhibited by corals with similar MPS levels, the simple shape standardisation used in Chapter 2 was undertaken for comparing mechanically disparate colonies. The "shape-index" of an observed colony on the reef was defined as the height to diameter ratio (S) of a solid cylinder that sustains the equivalent MPS at its basal attachment (see Chapter 2 for detail and Fig. 5.1 for the relationship between MPS and shape-index). The instantaneous rate of mortality

was then estimated for a range of colony shape-indices every four metres over the reef transect from the reef base (-24m) to the reef back (600m) (see Fig. 5.4b for reef profile).

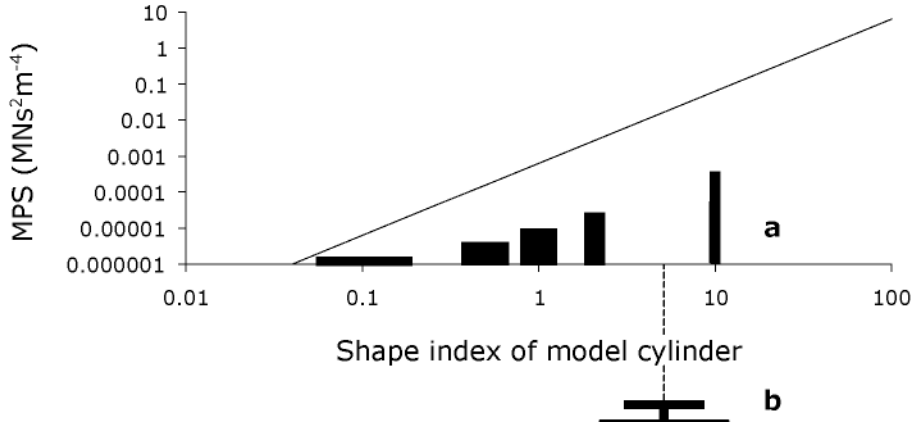

Fig. 5.1: a) Relationship between the shape index of model cylinder colonies and their MPS. b) An example of the approximate shape index of a tabular colony (e.g., *Acropora hyacinthus*) illustrating that projected area distributed closer to the substrate lessens internal mechanical stress.

5.2.4 The MPS of colonies from three local populations

MPS measurements were taken from colonies of three reef coral species that were abundant on the southeast reef at Lizard Island and exhibited different growth forms. The first species, *Acropora palifera* (subgenus Isopora), forms sturdy sub-massive mounds with the largest attachment area relative to colony size of the three focal species (Fig. 3.2a). The second species, *Acropora gemmifera*, forms corymbose (bushy) colonies with a solid, although geometrically variable, substrate attachment (Fig. 3.2b). The final species, *Acropora hyacinthus*, is fast-growing and forms horizontal tables up to several square metres in size, and is typically attached to the substrate by a short central stalk (Fig 3.2c). The growth characteristics of *Acropora hyacinthus* enable colonies to quickly overtop and shade slower growing species and, consequently, *Acropora hyacinthus* has been shown to be a dominant competitor in many exposed reef

crest habitats where, in the absence of regular hydrodynamic disturbance, it often forms monocultures (Stimson 1985; Baird and Hughes 2000).

The MPS and distance from the reef crest were recorded for all colonies of the three study species within six 80 x 2m belt transects extending from the crest shorewards towards the reef back (see Chapter 4 for details). Deeper water colonies were not sampled due to confounding influence of light on reef corals morphologies. Sampling was discontinued at 80m from the crest due to a significant decline in abundance of all three species which is characteristic of these crest-dwelling species in general. Two predicted mechanical thresholds were projected onto the study population dataset as a function of distance over the reef. The first threshold was estimated based upon extreme hydrodynamic disturbance, and was believed to have been imposed upon the population as a result of the largest hydrodynamic event during the past 37 years (cyclone Rona in 1999, Table 4.1). The second threshold was estimated based upon the maximum expected hydrodynamic event in a year to give an indication of the potential yearly turnover of individuals within the three study populations caused by hydrodynamic disturbance at the study site.

5.3 Results

5.3.1 Coral mortality resulting from hydrodynamic disturbance is a Poisson process

Coral mortality caused by hydrodynamic disturbance at Lizard Island was found to approximate a Poisson process. The model exponential distribution closely approximated the observed frequency distributions regardless of whether mortality events were frequent, as they were for colonies with a high shape index (e.g., a shape index of 12.5; Fig. 5.2a), or infrequent, as they were for colonies with a low shape index (e.g., a shape index of 5.5; Fig. 5.2d). An approximate fit of predicted and observed distributions justified the use of the fitted parameter μ as an estimate of the mean rate of colony dislodgement at the study site.

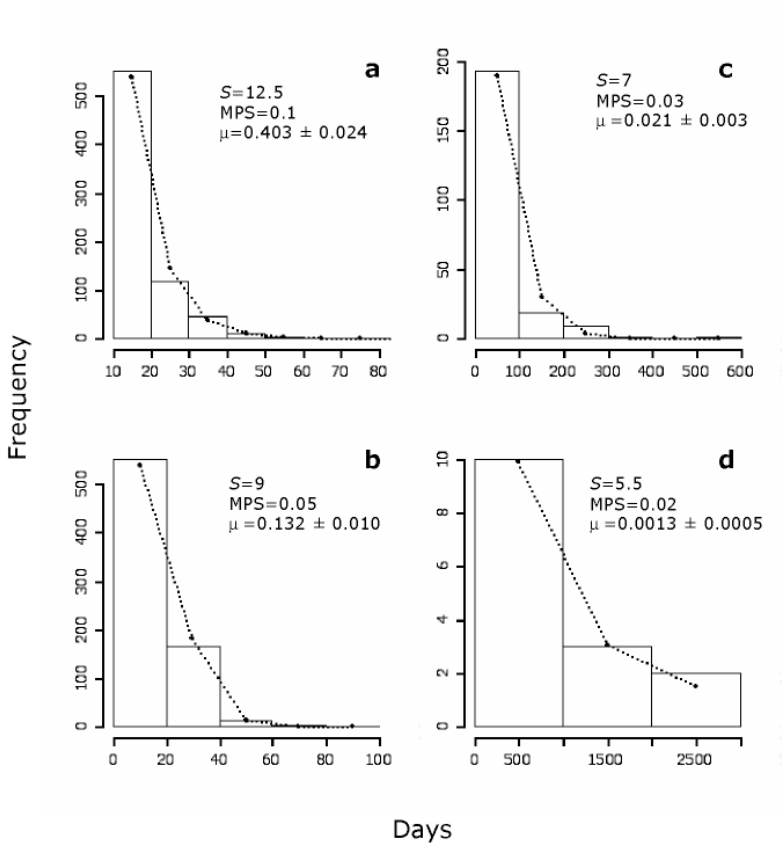

Fig. 5.2: Frequency distributions of waiting times between mortality events at the reef crest for four differently shaped colonies during the 37-year record of wave events at Lizard Island. Shape index (S), MPS (σ_{mps}) and best-fit mortality rate ($\mu \pm$ SE) are displayed for each calculation. Time is in log(days).

5.3.2 Variation in mortality rate over the reef

There was marked spatial variation over the reef in the estimated mean mortality rates for colonies with a given shape-index (Fig. 5.3). Variation was greater for mechanically stronger colonies (i.e., lower shape indices) and almost non-existent for the weaker colonies modelled. For example, a colony with a shape-index of nine would, on average, be predicted to survive approximately three orders of magnitude longer 40-60m back from the crest than it would at the crest, and greater than three orders of magnitude longer at the reef base. A mechanically weak colony with a shape-index of 56 would, for example, be predicted to survive for similarly short periods (i.e., approximately one day) regardless of where it grew over the reef transect (such as colony is unlikely to exist on a reef unless it is fully protected from water motion or structural supported).

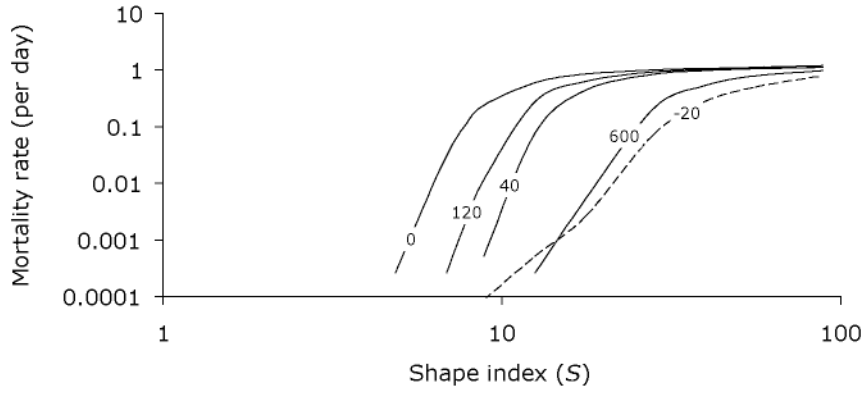

Fig. 5.3: Estimated mortality rate for a given colony shape index for five positions over the reef transect labelled as distance from the reef crest (see Fig. 5.4b for orientation on reef depth profile). Dashed line represents the reef base which displayed a substantially more gradual relationship between shape index and estimated mortality rate.

At a given zone over the reef, estimated mortality rate initially increased rapidly as a function of shape index, and then plateaued at a rate of approximately one event per

day (Fig. 5.3). However, the intercept of the mortality/shape curve with a given mortality rate differed substantially with respect to reef zone. An exception to the general relationship between mortality rate and shape-index occurred in deeper water (dashed line in Fig. 5.3) where the slope of the curve was more gradual and did not demonstrate a clear plateau. This pattern indicated a less pronounced effect of increased shape-index on mechanical vulnerability in deeper water habitats than on the shallower reef platform.

Variation in estimated mortality rate over the reef gradient identified three mechanical refuges in which relatively weaker colonies are predicted to be more likely to persist (Fig. 5.4). As expected, the reef base and reef back appeared to present two refuges where, for a given shape-index, mortality rates were substantially lower than in other reef zones. The relatively low mortality projections from disturbance were determined to be the result of reduced maximum water velocities at these positions. The third mechanical refuge was most prominent at 40-60m back from the reef crest, but did not reduce mortality estimates as much as did the reef base and reef back refuges (Fig. 5.4). To illustrate the relative influences of the three refuges, a colony with a shape index of 9 would be expected on average to be dislodged approximately once every 27 years at the reef base, every 3 days on the crest, every 3-4 months 50m back from the crest and every 30 years 450m back shorewards over the reef (Fig. 5.4).

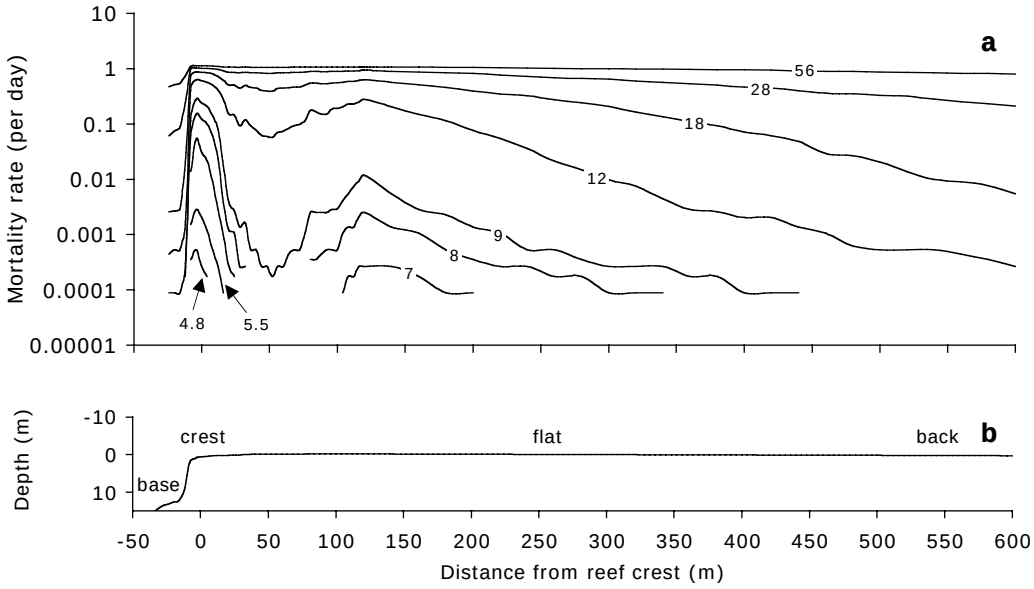

Fig. 5.4: a) Instantaneous rate of mortality for different colony shape indices over the reef transect, from the reef base (-24m) to the reef back (600m). Shape index is given for each contour. b) The reef depth profile as a function of distance from the reef crest; and generic names for different regions of the profile.

5.3.3 Projecting model mechanical thresholds onto real coral populations

Projection of estimated mechanical thresholds onto the MPS levels of colonies from the three focal coral populations illustrated clear differences in the potential mechanical threat posed by hydrodynamic disturbance at the study site. No colonies of *Acropora palifera* had MPS values greater than that which would have been predicted to have been mechanically dislodged following the single largest hydrodynamic event in the past 37-years at Lizard Island (cyclone Rona in 1999; solid line, Fig. 5.6a). It is therefore believed to be unlikely that hydrodynamic disturbance is a significant agent of mortality for this mechanically robust species on the southeast reef at Lizard Island. On the other hand, a number of colonies of *Acropora gemmifera* did fall above the 37-year threshold, thus indicating that colonies from this population may potentially be dislodged given a hydrodynamic disturbance similar to that projected (Fig. 5.6b).

Moreover, a few colonies of *Acropora gemmifera* fell above the one-year threshold (dashed line), which illustrated that this species may be subjected to yearly hydrodynamic mortality events that cull a relatively small portion of the population. In contrast to *Acropora palifera* and *Acropora gemmifera*, a significant proportion of the *Acropora hyacinthus* population fell above the 37-year threshold suggesting that, given an equally high disturbance regime in the near future, approximately a quarter of this population may be dislodged (Fig. 5.6c). Furthermore, the expected one-year mechanical threshold showed that a significant proportion of the *Acropora hyacinthus* population is likely to be removed by hydrodynamic disturbance on a yearly basis.

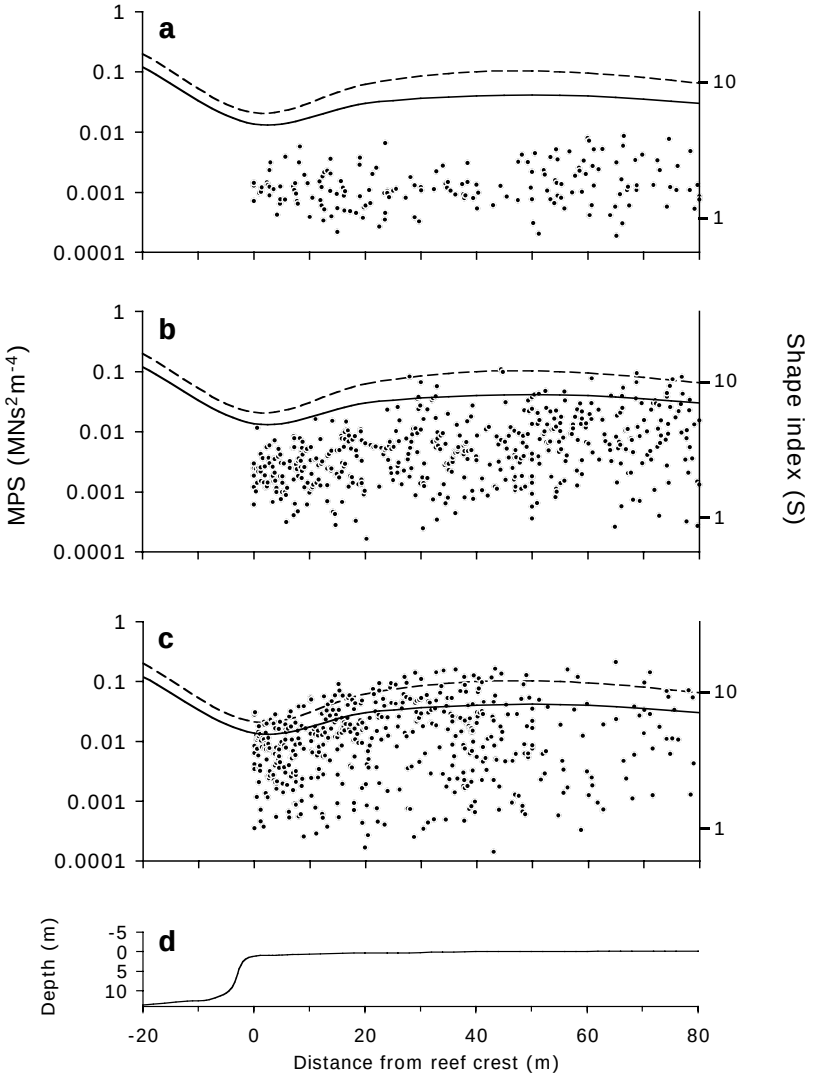

Fig. 5.5: a) Instantaneous rate of mortality and average time between mortality events for different colony shape indices to 80m over the reef transect. b) Empirical MPS levels and shape indices for colonies of *Acropora hyacinthus* ranging from the reef crest to 80m over the flat. The expected mechanical threshold in one year (dashed line) and the mechanical threshold produced by the largest wave event during the 37-year record, cyclone Rona in 1999. c) Average size of *Acropora hyacinthus* colonies measured as the average diameter of the horizontal plate (±standard errors). d) The reef depth profile.

5.4 Discussion

5.4.1 Hydrodynamic disturbance approximates a Poisson process

This study demonstrated that wait times between mechanically-induced mortality events at Lizard Island are approximately exponentially distributed, thus indicating that the disturbance frequency can be approximated as a Poisson process (i.e., one in which each disturbance event is random and independent; Spiegel 1992). Because many meteorological phenomena often closely approximate Poisson processes (Solow 1989), and because wind and wave regimes are implicitly related in fetch-limited water bodies (Komar 1997), this result was not unexpected. Nonetheless, this finding was critical to the overall study objectives in that it made possible the subsequent estimation of the predicted instantaneous rates of disturbance-induced mortality for coral colonies based on their mechanical vulnerability. Calculation of the Poisson coefficient μ from fitted exponential probability density functions resulted in estimates of the predicted mean instantaneous rate of mortality for colonies based on a measure of their mechanical integrity. This result therefore facilitates modelling of assemblage turnover on coral reefs.

5.4.2 Hydrodynamic disturbance and mortality

The steep increase in predicted mortality rate, which results from a relatively small increase in shape-index, was unexpected (Fig. 5.3). This finding suggests that, in theory, a relatively clear-cut threshold of mechanical vulnerability, which represents a dynamic balance between changes in colony vulnerability and disturbance regime through time, should exist for different coral populations. For example, at the reef crest, a branching colony with a shape-index of 5.5 would have an expected mean time

between mortality events of 3 years, whereas, a branching colony with a shape-index of 9 (less than twice as high as the first colony) would have an expected mean time between mortality events of once a week (Fig. 5.2d and b respectively).

Although the highest shape-index measured empirically in this study at the reef crest was approximately 6.9 (a colony of *Acropora hyacinthus* with $1/\mu = 56$ days), it is not uncommon to observe colonies at the study site that have much greater shape-indices. Four factors may permit higher than expected shape-indices. First, maximum water velocity over the reef was calculated using a depth-averaged reef profile (Chapter 4). Depth averaging removes local topographical variation, such as protrusions and depressions, simplifying colony-scale hydrodynamics, and is thus likely to moderate zones of greater or lesser maximum water velocity (Carstens 1968; Chapter 4). Secondly, mechanically vulnerable growth forms potentially increase their integrity by fusion of neighbouring colonies (e.g., haystacking of branching colonies and peripheral fusion of plating colonies; Tunnicliffe 1981; Chapter 2). In such cases, the whole structure should be defined as one mechanical entity. Third, substrate strength at the study site was found to range almost an order of magnitude about the mean (Chapter 2). However, most of this variation occurred at a spatial scale much smaller than a colony basal attachment area ($< 1cm^2$). Consequently, as multiple colonies grow and spread over the substrate, their individual limiting strength will approach the local substrate mean and differences in limiting strength between the individual colonies will decrease. Because a relationship between basal attachment area and substrate strength variability has not been established, the present study assumed that the basal attachment areas of the study colonies were sufficiently large that any variability about the local mean was minimal. However, it is likely that strength variability at the scale of colony basal area does exist (although it must be to be considerably smaller than the sampling variability),

which implies that there will be a nontrivial amount of variation in mean mortality rate for a given shape-index. That is, the estimated morality rate will vary to some extent for a given colony depending on its exact substrate strength, although this variability will be more pronounced in colonies with smaller attachment area. Fourth and finally, because mortality rates can only be calculated for colony shapes that are dislodged during the 37-year record, the approach represented here will only apply to the mechanically weaker subset of colonies on the reef. During the 37-year period, colonies with shape indices of 4.5 or lower were theoretically never dislodged at any position over the reef. This suggests that coral colonies with low shape indices are rarely dislodged on the exposed southeast reef of Lizard Island (e.g., hemispherical or encrusting morphologies), and for these animals other mortality agents are likely to be more important (such as competition, predation or disease; Hughes and Connell 1999). One relevant phenomenon which was not explored explicitly in this study was the weakening effects of bioerosion (Tunnicliffe 1981; Highsmith 1981). Measurements of skeletal and substrate strength in Chapter 2 implicitly included bioerosion and diagenetic processes. However, bioerosion may be more prevalent beneath coral colonies (Highsmith 1981; Schoenberg 1999). Such a phenomenon would increase a colony's chance of dislodgement and warrants further investigation.

Lizard Island had not been directly intercepted by a cyclone for at least the 37 years prior to this study (Chapter 4), and consequently the range of colony shapes for which mortality rates were calculated in this study represent a fraction of those that would be dislodged during a direct cyclone strike. The maximum horizontal flow velocity estimated at the study site's crest over the last 37 years was a moderate $3.6ms^{-1}$. Velocities of up to $12ms^{-1}$ have been recorded on rocky shores during severe wave events (Gaylord 1999), and estimates of maximum velocity have been made in excess

of 25ms^{-1} (Denny et al. 2003). These velocities are unlikely to exist in the GBR lagoon due to the blocking of oceanic waves by outer reefs and fetch-limitation of locally developed wave climates (Symonds et al. 1995). However, a conservative estimate based on wave climates developed by a category five cyclone near Lizard Island (winds of ~150kmh^{-1}) suggests that a direct strike could produce a maximum water velocity of approximately 8-10ms^{-1} at the reef crest (Shore Protection Manual 1984), a velocity sufficient to dislodge colonies with a shape index of 1.5 or greater (roughly isometric and similar to many hemispherical growth forms).

5.4.3 Magnitude of disturbance effects over the reef

The projected mortality rates of coral colonies from hydrodynamic disturbance differed markedly over the reef transect. The gradient in mortality over the reef was most variable for stronger colonies and increasingly less for colonies with higher shape-indices, even at the relatively benign reef base and reef back habitats (Fig. 5.2). This result suggests that the higher the colony shape-index, the greater the chance that *all* individuals of this index over the reef of being dislodged during a hydrodynamic disturbance. Conversely, the lower the colony shape-index (i.e., the more robust the colony), the more likely individuals will remain in mechanical refuges over the reef after significant hydrodynamic disturbances.

The crest community exhibited the highest predicted mortality rates for all colony shapes (Fig. 5.4a) even though the reef substrate there was strongest (Chapter 2). Differences in the two physical gradients over the reef (i.e., substrate strength and maximum water velocity) produced three clear mechanical refuges. Two of the refuges were not surprising: the base of the reef crest and reef back (Fig. 5.4a). The third refuge, which is previously undescribed on coral reefs, was located on the outer reef flat

and is apparent as a trough in the predicted mortality rate at approximately 50m back from the crest. This refuge was the result of two opposing physical gradients. The first, the gradient of maximum flow velocity, was always greatest near the crest during mechanically significant wave events and decayed in a roughly exponential fashion towards the reef back as waves attenuate over the reef (Hardy and Young 1996; Chapter 4). The second was a gradient in the degree of substrate cementation (Macintyre and Marshall 1988; Rasser and Riegl 2002; Chapter 2) which was also strongest at the crest and decays towards the reef back, albeit at a slower rate than that of the velocity gradient. Consequently, the mechanical refuge on the outer reef flat was found where flow velocity had attenuated significantly and the substrate was still relatively strong. Beyond this point, levels of flow velocity remained relatively constant and the substrate became increasingly unstable further towards the inner reef flat. Finally, substrate strength levelled off and flow velocity continued to attenuate, reducing mortality rates once more further towards the reef back.

Mechanical refuges potentially facilitate growth of mechanically weaker colonies and increase the potential for assemblages to reach more mechanically vulnerably levels of development than surrounding zones. At the Lizard Island study site, mechanical refuges tended to contain a greater number of high shape-index colonies and live coral cover was visibly greater (pers. obs.). The effects of these refuges on species diversity are unknown at this point, but would be an interesting basis upon which to examine the spatial effects of disturbance on a reef.

5.4.4 Mechanical thresholds

As with terrestrial plant assemblages, competitive dominance on coral reefs is often maintained by species that utilise vertical growth to overtop, and consequently shade,

understorey species (Jackson 1979). *Acropora hyacinthus* frequently attains dominance in exposed reef crest habitats (Stimson 1985; Veron 1993; Baird and Hughes 2000). In assuming a competitively dominant growth strategy, this species' mechanical integrity is sacrificed by growing up and over the top of neighbouring colonies while retaining a small basal attachment area. This growth strategy results in a clear power relationship between MPS and colony size (Chapter 3). This favourable competitive growth strategy therefore represents a classical trade-off between competitive ability and mechanical stability (Connell 1978; Jackson 1979; Grimes 1980).

For *Acropora hyacinthus*, the upper limit of structural susceptibility (MPS) varies strongly with location on the reef transect. Projecting the mechanical threshold expected to have been imposed during the last major hydrodynamic event (cyclone Rona 1999, Chapter 4) resulted in a projected upper limit to MPS values that conformed to upper limit of the empirical distribution of colonies over the reef. Moreover, the presence of points above the projected mechanical threshold is precisely what would be expected if colonies have subsequently begun growing after the last significant disturbance.

This chapter synthesised the previous three chapters by presenting a spatially explicit framework for quantitatively predicting the size-selective and shape-selective nature of hydrodynamic disturbance on coral reefs. With knowledge of the characteristic levels of MPS within colonies of different species and how these levels change with size, it was possible to estimate which colonies are more likely to be dislodged over the reef. The utility of this approach in modelling community dynamics will be discussed further in the final chapter. Globally, the intensity and frequency of storm and cyclonic events are expected to change based on current climate change projections (Henderson-Sellers et al. 1998; Nott and Hayne 2001; Walsh et al. 2001).

Therefore, modelling approaches that incorporate accurate estimates of hydrodynamic disturbance and its effects on coral colonies may afford greater insight into the long-term dynamics of reef assemblages.

CHAPTER 6: General discussion

Through the integration of engineering, morphological and oceanographic approaches and their subsequent application to an ecological question, this thesis has demonstrated that the mechanistic prediction of hydrodynamic disturbance on reef coral assemblages is not only possible, but is also critical to the development of a more robust understanding of the fundamental mechanisms driving reef community dynamics. A number of key findings of this thesis form the basis for this conclusion. This chapter summarises these findings, relates them to previous research in this area, and subsequently discusses the benefits of the development of this mechanistic framework for understanding and predicting the effects of physical disturbance in coral reef communities.

6.1 The biomechanical limitations of corals

The present study integrated classical engineering theory with a geometric model of a coral colony to illustrate that the tensile strength of a coral's colony/substrate interface is the limiting factor in determining a colony's ability to contend with the forces exerted by water motion (Chapter 2). For the vast majority of species explored, the tensile strength of coral skeleton was substantially stronger than the substrate to which they are attached. This finding suggests that substrate strength, in general, limits overall colony integrity (defined here as the ability to withstand hydrodynamic force) (Fig. 2.4). Moreover, the disparity between skeletal strength and substrate strength was much greater for mechanically vulnerable colony morphologies, such as branching or

tabular colonies, indicating that substrate strength may be significantly more limiting for species which are more likely to be dislodged by hydromechanical forces.

Although substrate from only one reef was examined in this study, previous research indicates that the substrate strengths found in this study are typical of other reefs in the Great Barrier Reef lagoon (Foster 1974; Chapter 2). An early exploratory study by Foster (1974) examined the strength of coral reef substrate at a latitudinally-central GBR reef with the aim of determining the suitability of coral reef platforms as a substrate for the construction of man-made engineering structures (e.g., tourist pontoons). This study utilised the same geomechanical method as was used in the present study (dynamic cone penetrometry), therefore the results obtained by Foster (1974) can be directly compared to those found here. As can be seen in Fig. 2.4, substrate strengths found in the two studies were not substantially different, with a relative difference of approximately 8% between the mean substrate strengths. This similarity in substrate strength suggests two things. First, the values obtained for substrate strength in this thesis are not anomalously low. Secondly, this similarity supports the general applicability of these findings to other geographical areas. The substrate strength values found by Foster (1974) were somewhat lower than those found in this study, suggesting that the estimates from Lizard Island are conservative and may slightly overestimate the strength of coral reef substrate elsewhere. This comparison therefore lends further support to this study's conclusion that substrate strength is, in the vast majority of cases, the limiting material in determining a coral colony's overall ability to withstand hydrodynamic force.

The implications of this finding are particularly important to ecological projections of coral response to disturbance. Past research has attempted to make such predictions based on coral skeletal strength. These studies did not consider the possibility that, as

has been shown in the present study, reef substrate material may serve as the "weakest link" in determining colonies' overall strength. Three published studies (Chamberlain 1978; Schuhmacher and Plewka 1981; Vosburgh 1982) have examined various mechanical properties of scleractinian coral skeletal material, and, based on their findings, each assumed that the skeletal strength was the general cause of mechanical failure in these animals when exposed to hydrodynamic disturbance. Chamberlain (1978) was the first to quantify the mechanical properties of coral skeleton and to suggest how these properties may influence ecological zonation on the reef. In this study, Chamberlain (1978) measured the compressive and bending strengths of coral skeleton from three coral species and, in agreement with this thesis, found that skeletal material was stronger in more mechanically vulnerable growth forms (e.g., branching and tabular growth forms; Chapter 2). However, Chamberlain (1978) failed to consider the mechanical properties of the substrate to which corals are attached, and therefore may have significantly overestimated the overall integrity of colonies of these species. More importantly, his study may have overestimated the differences between overall colony strength between species by basing his conclusions on skeletal strength. In a subsequent study, Massel and Done (1993) used Chamberlain's (1978) estimates of one coral species' limiting strength in a study of the survival probabilities of large hemispherical coral species on the GBR. Because of the potentially erroneous assumptions (described above) upon which they based their study, Massel and Done (1993) are also likely to have overestimated the strength of coral colonies. They concluded that hemispherical colonies would never be dislodged from the reef unless their colony/substrate adhesion area was almost completely eroded by bioerosion. Schuhmacher and Plewka (1981) and Vosburgh (1982) undertook similar studies on the mechanical properties of coral skeleton to that of Chamberlain (1978). These studies

also concluded that the inherent mechanical differences between their study species may potentially influence their ecological distribution through different levels of vulnerability to hydrodynamic disturbances, yet once again this study failed to consider the strength of the substrate to which their study species were attached. For these reasons, the conclusions found by these previous studies support the present study's conclusions of relative differences in overall strength between coral species, but their findings on absolute colony resistance to dislodgement by hydrodynamic force are likely incorrect.

Bioerosion is a potentially important phenomenon that is likely to significantly weaken the materials at the colony/substrate interface (Chamberlain 1978; Tunnicliffe 1979; Highsmith 1981; Highsmith et al. 1983). The present study approached the question of material strength in two parts so as to implicitly include the effects of bioerosion in weakening measurements of material strength. First, using non-eroded skeletal cores, the relationship between uneroded skeletal strength and density was established. Secondly, a reef-wide collection of coral skeletal samples from the three focal species was made and the densities of these samples were converted into strength using the strength/density relationship established in the first part of the study. This procedure ensured that coral samples that were bioeroded (and consequently had lower densities than uneroded samples) would result in lower strength estimates than the uneroded samples. Furthermore, the geomechanical technique used to measure the strength of the substrate (substrate probing) also inherently accounted for the effects of bioerosion because there was no discrimination between eroded and non-eroded areas of reef substrate. Therefore, although bioerosion was not explicitly measured in the study samples, the methods used have implicitly accounted for these effects.

Nonetheless, the indirect inclusion of bioerosion in this study may not be sufficient to account for unknown differences in the extent of bioerosion at the colony/substrate interface as a function of species, size and position of the reef. For example, in a study examining bioerosion by boring sponges (which are often responsible for the majority of bioerosion on coral reefs; Highsmith 1981), Schoenberg (2002) found significantly different rates of bioerosion within different coral species and, therefore, suggested that the extent of bioerosion is likely to be greater and more variable in longer-lived larger colonies. Highsmith et al. (1983) found that bioeroders (e.g., sponges, boring bivalves, etc.) tend to erode skeletal material more in the internal regions of the colony and less in the outer regions, where second moments of area are substantially less pronounced. This finding is important because the outer regions of the colony account for the vast majority of resistance to mechanical stresses (Wainwright et al. 1982; Chapter 2). Although bioerosion does play a role in weakening skeletal strength, the decrease may not be directly proportional to the amount of material eroded. However, the degree to which excavation at the colony/substrate interface differs as a function of colony size and of taxonomic identity, and how it may affect mechanical integrity, is largely unknown and would be a useful avenue for future research.

6.2 The dominant hydrodynamic force acting on coral colonies

Three different types of hydrodynamic force act, to varying degrees, on a coral colony exposed to water motion: drag and lift, which are produced by water velocity, and inertial force, which is produced by water acceleration. Vogel (1996), in a theoretical evaluation of these three forces, suggested that for the typical size of benthic animals and plants ($1cm^2$ to $1m^2$ projected area) and the maximum water motion to

which they are exposed (often greater than $10ms^{-2}$), the contribution of drag force to the total force upon an organism was substantially larger than either of lift or inertial forces (i.e., for Reynolds Numbers between 10^3 and 10^5). In another interpretation of hydrodynamic forces acting on coral colonies, Massel and Done (1993) found that inertial force, caused by the acceleration of water, could potentially be as much as an order of magnitude greater than drag force, and was thus likely to be more important to coral mechanical integrity. Their study, however, differed from the present study in that they modelled only the largest subset of coral colonies that are found on coral reefs (i.e., those which are greater than $1m^2$ projected area), for which inertial forces become increasingly more prominent. In a theoretical summary of the relative importance of hydrodynamic forces on sessile organisms, Denny et al. (1999) concluded that, in accordance with this thesis (Chapter 2), drag processes produce the maximal force acting on the range of macroscopic sessile organisms found in wave-swept habitats. Therefore, because drag force is directly proportional to water velocity (Gerhart et al. 1992), it is the maximum level of the horizontal velocity component of wave motion that exerts the majority of hydrodynamic force on a colony.

6.3 Predicting the maximum stress at the colony/substrate interface

The magnitude of tensile stress at a coral's basal attachment produced by drag force is (for a given water velocity) a function of the projected shape of the colony's morphology perpendicular to water motion, and is not necessarily a function of the colony size per se (i.e., similarly shaped colonies of different sizes may experience the same maximum mechanical stresses; Chapter 2). Because the velocity-induced drag force acting on a colony is directly proportional to the colony's horizontal projected

area (Denny 1988; Vogel 1996), colony area further from the substrate contributes more to bending the colony about the substrate than area closer to the substrate. This force, summed over all colony area, subsequently produces tensile stress in the colony's base (Denny 1988, Chapter 2). Therefore, greater proportional distribution of area away from the substrate leads to more concentrated levels of tensile stress at the colony/substrate interface (Fig. 3.2). This growth pattern is typified by the tabular study species *Acropora hyacinthus,* a species which generally increases its mass in greater proportion in the regions farther from the substrate but does not compensate mechanically for this distribution by, for example, increasing its girth to dilute internal stresses. Consequently, a colony's distribution of its projected area (i.e., its shape) is the primary factor that determines mechanical integrity, and this factor is one over which individual colonies and coral species may potentially have some degree of ecological or evolutionary control (Graus et al. 1977; Oliver et al. 1983; Kaandorp 1999; Chapter 2).

Previous studies of the mechanical effects of hydrodynamic disturbance on coral assemblages (Graus et al. 1977; Massel and Done 1993) indicate the ecological importance of mechanical differences between species and between colonies of the same species. Using digitised images of colonies' outlines and the biomechanical theory outlined in Chapter 2, I developed a novel mechanical technique for quantitatively predicting the maximal tensile stress that a colony exerts on the substrate for a given water velocity (the maximum predicted stress [MPS]; Chapter 3). Measurements of the MPS of colonies from the three focal species at the exposed southeast reef platform at Lizard Island illustrated that mechanical vulnerability depends strongly on taxonomic identity, colony size and position over the

hydrodynamic exposure gradient which is characteristic of exposed shallow reef platforms.

6.3.1 Maximum predicted stress as a function of taxonomic identity

Comparisons of MPS levels between the three study species were striking. Tabular colonies of *Acropora hyacinthus* displayed average levels of MPS substantially greater than corymbose *Acropora gemmifera* colonies which, in turn, had MPS levels much greater than the sub-massive species *Acropora palifera* (Fig. 3.2). For example, given the same limiting substrate strength, an average colony of *Acropora palifera* can theoretically withstand a flow velocity 20-times greater than *Acropora hyacinthus*, illustrating clear species differences in the potential for dislodgements during hydrodynamic disturbances (Chapter 2). These results fit well with those of previous studies that have recorded differences in interspecific colony dislodgement following cyclonic wave climates. In a survey of coral dislodgement and damage at previously established study sites following a hurricane (cyclone) in Jamaica, Woodley et al. (1981) found that differences in damage to different growth forms were particularly striking for corals. At one site, cover of *Acropora spp*. (tabular and branching growth forms) had been reduced by up to 99%, whereas hemispherical growth forms of various other species (e.g., Porites, Mussids and Favids) had been reduced by only 9% (Woodley et al. 1981). Similarly, through a long-term dataset of coral demographics at Heron Island (GBR), Connell and Hughes (1999) were able to quantify damage attributable to cyclones and found a ten-fold difference in the percent reduction of coral cover between tabular (42%) and hemispherical (4%) growth forms. Both of these studies demonstrate differences in mechanical vulnerability between relatively delicate and robust morphologies as predicted by the present study.

6.3.2 MPS as a function of intra-specific colony size

Chapter 2 argued that mechanical vulnerability should be directly related to colony shape and should be independent of colony size, yet clear changes in MPS with size were found for two of the study species (*Acropora hyacinthus* and *Acropora gemmifera*; Fig. 3.4). However, this unexpected relationship occurs because of changes in shape of colonies as these two species grow. Importantly, this relationship therefore demonstrated an indirect influence that size may have on mechanical vulnerability for some species (Chapter 3), and this finding should be explicitly considered in future studies of this nature. Furthermore, the three study species showed three distinct patterns in the relationship between size and mechanical vulnerability (Fig. 3.3). *Acropora palifera*, demonstrated no obvious relationship between colony size and mechanical vulnerability. This result is likely to be the consequence of isometric growth, so that an increase in internal stress, caused by an increase in a colony's projected area, is counteracted by a corresponding increase in basal area over which that internal stress is distributed (Fig. 2.3). Therefore, in support of the conclusions of the geometric model developed in Chapter 2, this lack of a relationship shows that colony size is not an important determinant of mechanical vulnerability to hydrodynamic force for species with approximately isometric characteristic growth strategies (e.g., hemispherical growth forms). This conclusion is further supported by the presence of large hemispherical colonies which have been observed to successfully grow in a wide range of hydrodynamic reef habitats (e.g., Barnes and Lough 1992; Veron 1993).

Acropora hyacinthus, showed a distinct relationship between mechanical vulnerability and colony size in which large colonies consistently exhibited higher levels of MPS than smaller colonies. This relationship was the result of the vertical and

lateral growth seen in tabular-shaped colonies which was not matched by a corresponding increase in the basal attachment area necessary to counter internal stresses. Other growth forms in which height or width increase allometrically with basal width, such as branching species, are likely to exhibit a relationship between size and mechanical vulnerability which is similar to that of *Acropora hyacinthus*.

A third pattern, illustrated by *Acropora gemmifera*, was a combination of the relationships between colony size and mechanical vulnerability exhibited by *Acropora palifera* and *Acropora hyacinthus*. This pattern demonstrated that mechanical vulnerability was potentially, but not necessarily, a function of size, and thus suggested the potential in some species for greater levels of morphological variability as colonies grow larger (e.g., Kaandorp 1999). Taken together, the relationships between colony size and mechanical vulnerability described above indicate that during a hydrodynamic disturbance, species which change shape as they grow should theoretically exhibit different levels of dislodgement across size classes. On the other hand, species whose shape changes little with growth should theoretically be dislodged independently of size (Fig. 3.5). This finding is critically important to understanding the effects of hydrodynamic disturbance upon coral community structure, but is extremely difficult to test empirically. For example, to capture differential dislodgement regimes of population size-structure during hydrodynamic events, which are rare and unpredictable relative to the duration of a typical research project (White and Pickett 1985), extensive long-term field studies are required. The few long-term ecological studies that focus on the long-term dynamics of these communities measure changes over relatively small spatial areas (e.g., 10m transects and 2m quadrats; Dollar and Tribble 1993; Connell et al. 1997). These sample areas provide insufficient sample sizes to investigate changes in population size-structure of species resulting from hydrodynamic disturbances and

thus cannot be used to empirically test the predictions of this thesis. As mentioned above, to properly test predictions of differential dislodgement regimes during a hydrodynamic disturbance would require a quantitative mechanical survey of corals both immediately before and immediately after the disturbance event. It is therefore suggested that future long-term studies of this nature consider this need and attempt to incorporate such before/after disturbance surveys into their study design.

6.3.3 Maximum predicted stress as a function of position along a hydrodynamic gradient

The study site's hydrodynamic gradient extends from the exposed reef crest over the increasingly sheltered reef flat and offered a template upon which spatial differences in mechanical vulnerability were examined. The three study species displayed vastly different patterns in their relationship between colony MPS and distance over the reef (Fig. 3.4). Mechanically robust colonies of *Acropora palifera* showed no clear relationship. This pattern was likely the result of characteristically low levels of MPS in this species and further suggests that colonies of this species, on average, are relatively mechanically resistant to the hydrodynamic disturbance regimes characteristic of reef platforms. Conversely, the corymbose colonies of *Acropora gemmifera* displayed an increase in variability in MPS of colonies as a function of distance from the reef crest, thus forming a wedge-shaped distribution of data points. This result suggests that colonies of this species may be mechanically constrained closer to the reef crest (Fig. 3.4b). The frequency distribution of *A. gemmifera* colony MPS levels over the reef was lognormal, with a standard deviation that increased linearly away from the reef crest. These patterns are consistent with morphological plasticity caused, at least to some degree, by the hydrodynamic habitat in which *Acropora gemmifera* resides.

Morphological variability along physical gradients is a ubiquitous phenomenon in scleractinian corals (Dunstan 1975; Veron and Pichon 1976; Graus et al. 1977; Oliver et al. 1983; Kaandorp 1999). For example, Graus et al. (1977) measured the inclination of *Acropora palmata* branches to align parallel with water motion over a hydrodynamic gradient. This thesis found a striking trend in which colonies exposed to strong wave action aligned with wave motion, while those in low-energy wave regimes showed no overriding branch distribution. In general, observed changes in growth form are, to some degree, a function of adaptation to light exposure and water motion (Oliver et al. 1983). The present study, however, controlled for the potentially confounding effect of light by restricting the focal area to the constant-depth reef flat. Therefore, by eliminating this potentially confounding source of variability, water motion can be concluded to be the most likely cause of the morphological variability seen in *Acropora gemmifera*.

The mechanically-weakest of the three study species, *Acropora hyacinthus*, also displayed an increase in variability in colonies' MPS levels as a function of distance over the reef. However, in contrast to *Acropora gemmifera*, truncation of higher MPS colonies of *Acropora hyacinthus* from a lognormal distribution was detected and was increasingly pronounced closer to the reef crest (Fig. 3.4c). A clear point of truncation of colonies with MPS greater than the predicted mechanical survival threshold strongly suggests that the *Acropora hyacinthus* population had been shaped by a mechanical threshold exerted by a past hydrodynamic disturbance. As one of the fastest growing coral species in terms of planar coral cover (Stimson 1985), colonies of *Acropora hyacinthus* would interact with an on average lower level of hydrodynamic activity per unit of colony growth than would, for example, *Acropora gemmifera*. Consequently, *Acropora hyacinthus* may be less likely to grow under the constraints of their

hydrodynamic habitat (Kaandorp 1999). Therefore, as one of the most competitively successful growth strategies on the reef (Jackson 1979; Stimson 1985; Baird and Hughes 2000), the growth form of *Acropora hyacinthus* appears to be an example of the classic trade-off between mechanical integrity and competitive ability (Chapter 3). For example, in the absence of intense hydrodynamic disturbances, colonies of *Acropora hyacinthus* may have sufficient time to growth into larger competitively dominant colonies which can outcompete neighbouring corals by overtopping them, and can also pre-empt future competition by reducing access to substrate available for coral recruitment (Stimson 1985; Baird and Hughes 2000). On the other hand, intense and/or frequent hydrodynamic disturbance regimes will exert a lower mechanical threshold upon the size to which colonies can grow, and thus will likely reduce the abundance of individuals in larger size-classes. Subsequently, such a mechanical threshold may reduce the competitive influence of *Acropora hyacinthus* in reef communities and increase the potential for the recruitment and growth of competitively subordinate species (Connell 1978).

Having delineated the effects of shape, size and location on the mechanical vulnerability of individual coral colonies, this thesis found evidence for three distinctly different biomechanical strategies that are likely to be primary determinants of coral assemblage dynamics (at time scales which include recurrent hydrodynamic disturbances). The concept of periodic disturbance increasing the potential for interspecific coexistence within a community, by removing competitive dominants, is well known (e.g., Connell 1978). For this reason, the patterns found by exploring the application of maximum predicted stress developed in Chapters 2 and 3 prompted an investigation of the waiting times between hydrodynamic events large enough to dislodge colonies. I hypothesized that it would be possible to estimate the predicted

mortality rate of corals attributable to hydrodynamic disturbance with knowledge of how often water velocity on the reef exceeds the predicted mechanical limitations of a given colony.

6.4 Predicting colony dislodgement rates

Through quantitative investigation of the three factors that determine a colony's integrity (substrate strength, colony shape and water velocity), this thesis culminated in the estimation of the predicted dislodgement rates under the hydrodynamic disturbance regime in the Lizard Island region. Because the fragments of a dislodged colony can sometimes reattach to the substrate (Tunnicliffe 1982; Smith and Hughes 1999), dislodgement does not necessarily imply total colony mortality. However, dislodgement rates arising from extreme events were reasonably assumed to provide an estimate of coral mortality caused by hydrodynamic disturbance.

To estimate the instantaneous rates of individual colony mortality, this thesis used a 37-year meteorological record of the Lizard Island region and oceanographic models to back-project the hourly maximal water velocities which would have occurred spatially over the reef (Chapter 4). Using this back-projection, the wait times were calculated between hydrodynamic events with water velocities greater than those which colonies could theoretically withstand (based on their MPS values and the strength of the substrate to which they were attached; see Eq. 5.1). By fitting the distribution of wait times to an exponential model, it was found that potential colony dislodgement induced by hydrodynamic disturbance approximates a Poisson process (Chapter 5). Therefore, by calculating the instantaneous Poisson rate of change (Spiegel 1992), this study

predicted instantaneous mortality rate for individual coral colonies, based their mechanical integrity.

The only other known study that has explored the probability of coral colony survival in the context of mechanical vulnerability was that of Massel and Done (1993). However, their study was limited in its potential for modelling the effects of hydrodynamic disturbance on coral assemblages because a) they considered only one, relatively mechanically-resistant, growth form (i.e., hemispherical *Porites* colonies which are similar in shape but much larger than *Acropora palifera*), b) they overestimated the limiting strength of colonies by using compressive measures of skeletal strength by Chamberlain (1978), and c) they modelled colonies in relatively deep habitats (3-12m) where hydrodynamic forces are substantially weaker and cause less destruction (e.g., Woodley et al. 1981; Chapter 4). Therefore, it was not surprising that Massel and Done (1993) concluded that massive *Porites* species were immune to mechanical dislodgement by hydrodynamic disturbance unless colonies were separated from the substrate by bioerosion, and that gravitational force was the primary mechanism preventing a colony from toppling over (Fig. 2.9, Chapter 2). Consequently, their approach is not directly relevant to the biomechanical framework presented in the present study or for future modelling efforts on multi-species responses to hydrodynamic disturbance.

By superimposing the mechanical thresholds expected in one year and 37 years onto the measures of MPS of the three study species over the reef gradient, an estimate of the proportion of the existing populations that may be dislodged from the reef under these two hydrodynamic regimes could be approximated (Fig. 5.6). Results suggested that *Acropora palifera* does not face any significant risk of mechanical dislodgement on the southeast reef at Lizard Island, even on the relatively hostile reef crest. However,

the upper band of MPS in colonies of *Acropora gemmifera* lay between the one-year and 37-year projections, thus indicating the potential for these colonies to be dislodged during future disturbance regimes. In striking contrast to *Acropora palifera* and *Acropora gemmifera*, many colonies of the fast-growing, mechanically vulnerable species *Acropora hyacinthus* appeared above the one-year threshold, and approximately one third of the measured population was above the 37-year threshold. The presence of colonies above these mechanical thresholds indicates that colonies are likely to be culled from this population on a regular basis and, therefore, that mortality caused by mechanical dislodgement is likely to be a significant source of mortality for this species (Fig. 5.6c). Moreover, because of the clear relationship between colony size and mechanical vulnerability displayed by *Acropora hyacinthus*, mortality inflicted by hydrodynamic disturbance is likely to target the larger subset of the population on the reef (Chapter 3). Most importantly, the projections of potential mechanical thresholds onto this species closely mirrored the upper bound of the spatial pattern in MPS over the reef. Although no studies currently exist with which to compare these results, the similarity between the upper bound of MPS exhibited by colonies and the mechanical threshold generated by wave attenuation over the reef suggest that the approach used in this study adequately captured the factors which are fundamental to coral biomechanics.

Dislodgement rates of colonies based on a measure of their shape (MPS) were calculated spatially over the hydrodynamic reef gradient, producing a "contour map" of potential rates of mortality from dislodgement (Fig. 5.4). Given knowledge of a colony's MPS or shape-index, which can be calculated using a simple photographic technique (Chapter 3), the theory that produced this map facilitates the objective approximation of any colony's mean expected mortality rate caused by hydrodynamic disturbance at any position over the reef platform. Given sufficient information on the

relationship(s) between coral abundance and abundances of associated organisms, this method may also potentially allow for the quantification of the dynamics of the wider community resulting from hydrodynamic disturbance.

The three study species included in this study present a competitive hierarchy in which a) the dominant is mechanically weaker than the subordinates, b) the average geometric growth rates and background mortality rates are either available or potentially derivable from long-term monitoring of quadrats (e.g., Tanner et al. 1994), and c) recruitment potential may be related in free habitat space, depending on whether the supply of recruits is limited or not (Connell et al. 1997; Hubbell 1999). These factors create the potential for different modelling approaches (e.g., spatially explicit and individual-based or stage-structured matrices) to explore the dynamics of the three most abundant species on the shallow exposed reef at Lizard Island when mechanically inferior individuals (in this case the competitive dominant) are periodically removed from the assemblage. By including mortality caused by infrequent and destructive events, such models can potentially elucidate the relationship between hydrodynamic disturbance regimes and patterns of space formation (Levin and Paine 1974; Sousa 1984; Pickett and White 1985), species coexistence (i.e., the intermediate disturbance hypothesis; Connell 1978; Sheil and Burslem 2003) and associated changes in community processes such as recruitment potential (Connell et al. 1997).

Given recent suggestions that the intensity and frequency of cyclonic events may change as a result of global climate change (Mitchell et al. 1990; Houghton et al. 1996; Henderson-Sellers et al. 1998; Nott and Haine 2001), the development of a novel mechanistic framework for predicting the mechanical effects of disturbance in ecosystems is a timely and highly relevant undertaking. An increase in the frequency of cyclones will decrease the recovery time of coral assemblages, whereas a decrease in

cyclone frequency will allow time for greater potential competitive exclusion of competitive subordinates by dominant species. An increase in the intensity of cyclones will subject coral assemblages to lower mechanical thresholds and thereby constrain the growth of mechanically vulnerable growth forms, whereas a decrease in cyclone intensity will allow mechanical vulnerable species to reach greater sizes and potentially dominate reef habitats. Although there is no direct evidence that the frequency of cyclones has changed significantly in the recent past, recent studies indicate that the maximum potential intensity of cyclones may undergo a modest increase of up to 10-20% (Houghton et al. 1996). In summary, the framework developed in this thesis offers the ability to estimate the frequency and intensity of hydrodynamic disturbance, the impact that such events have upon coral colonies spatially across a reef, and the species-specific and size-specific mortality caused by those forces. By generating the appropriate models for measuring the dynamics of the coral reef system, such an approach will potentially facilitate projections of coral reef communities under past or future meteorological regimes.